DOI:
10.1242/dev.180075

Document Version
Peer reviewed version

Temporospatial sonic hedgehog signalling is essential for neural crest-dependent patterning of the intrinsic tongue musculature

Shigeru Okuhara [1*], Anahid A. Birjandi [2*], Hadeel Adel Al-Lami [2, 4], Tomoko Sagai [3], Takanori Amano [3, 5], Toshihiko Shiroishi [3], Guilherme M. Xavier [2], Karen J. Liu [2], Martyn T. Cobourne [2#], Sachiko Iseki [1#]

[1] Section of Molecular Craniofacial Embryology, Graduate School of Tokyo Medical and Dental University, Tokyo, Japan

[2] Centre for Craniofacial and Regenerative Biology, Faculty of Dentistry, Oral and Craniofacial Sciences, King's College London, London, United Kingdom

[3] Mammalian Genetics Laboratory, National Institute of Genetics, Mishima, Japan

[4] Present address: Department of Orthodontics, College of Dentistry, University of Baghdad, Iraq

[5] Present address: Next Generation Human Disease Model Team, RIKEN BioResource Research Center, Tsukuba, Japan

[6] Present address: RIKEN BioResource Research Center, Tsukuba, Japan

*** These authors contributed equally to this work**
 # Corresponding authors

ABSTRACT

The tongue is a highly specialized muscular organ that requires a complex anatomy for normal function. We have utilized a series of genetic approaches to investigate local temporospatial requirements for Sonic hedgehog (SHH) signalling during tongue development. Mice lacking a *Shh cis*-enhancer *MFCS4* (*Shh*$^{MFCS4/-}$) with reduced SHH from dorsal tongue epithelium have perturbed lingual tendon formation and disrupted intrinsic muscle patterning, with these defects reproduced following global deletion of *Shh* specifically from E10.5 in *pCag-CreER*^{TM}*;Shh*$^{flox/flox}$ embryos. SHH responsiveness was diminished in local cranial neural crest cell (CNCC) populations in both mutants, with SHH targeting these cells through the primary cilium. CNCC-specific deletion of the orofaciodigital syndrome 1 (*Ofd1*)-encoding ciliary protein in *Wnt1-Cre; Ofd*$^{fl/Y}$ mice produced a complete loss of normal myotube arrangement and hypoglossia. In contrast, mesoderm-specific deletion of *Ofd1* (*Mesp1-Cre; Ofd*$^{fl/Y}$) resulted in orderly arranged intrinsic lingual muscles. Collectively, these findings suggest key temporospatial requirements for local SHH signalling in tongue development; specifically, differentiation of the lingual tendon and patterning of the intrinsic musculature through signalling to CNCC and provide further mechanistic insight into the tongue anomalies seen in patients with disrupted Hedgehog signalling.

INTRODUCTION

The tongue is a highly specialized muscular organ situated in the oral cavity and upper pharynx of vertebrates that contributes to a number of essential functions including airway maintenance, phonetic articulation, oral sensation, mastication and swallowing. The significant morphological and functional variation seen in the tongue of vertebrates is reflective of multiple environmental adaptations amongst these organisms (Iwasaki, 2002). Normal function of the tongue requires the coordinated activity of both extrinsic and intrinsic muscles and their associated tendons, an extensive vasculature and complex motor and sensory innervation.

In the mouse embryo, tongue formation is heralded by the appearance of paired buds situated on the oral side of the first pharyngeal arch at around embryonic day (E)10.0. These buds grow and ultimately fuse with a medial lingual swelling to produce an early tongue primordium situated in the midline within the floor of the oral cavity by E11.0. The primordium is initially populated by cranial neural crest cells (CNCC) (Han et al., 2012); however, myogenic progenitor cells subsequently populate this region from E11.5, following their migration from the caudal occipital somites as the hypoglossal cord (Noden 1983, Czajkowski et al., 2014). Further development of the tongue requires interactions between the overlying oropharyngeal epithelium, CNCC and myogenic progenitors to regulate cell proliferation and differentiation. By E13.5 a prototype tongue structure is established, with symmetrically arranged intrinsic muscles connected by tendons, including a midline lingual septum (or *aponeurosis linguae*) within the tongue dorsum and a specific group of extrinsic muscles, which suspend the tongue between the skull, palate, mandible and hyoid (Han et al., 2012). Although the gross embryological processes have been understood for many years, it is only relatively recently that some insight has been gained into the complex molecular signalling events that coordinate these processes (Parada et al., 2012).

Disruption of canonical Transforming Growth Factor Beta (TGFβ) signalling in CNCC through loss of TGFβ-receptor 2 (TGFβr2) in mice results in microglossia secondary to abnormal myogenic precursor cell proliferation and organization, and connective tissue defects (Hosokawa et al., 2010). It has been suggested that the muscle defect is induced primarily through loss of Fibroblast Growth Factor 10 (FGF10) (Hosokawa et al., 2010) whilst the differentiation and proliferation of CNCC and their ability to induce other FGF's and Bone Morphogenetic Protein (BMP) signalling is also disrupted (Hosokawa et al., 2010, Iwata et al., 2013). These effects are also in part, mediated through non-canonical TGFβ signalling, which also regulates FGF10 through TGFβ-activated kinase (TAK1) (Song et al., 2013) and FGF/BMP signalling through the tyrosine-kinase ABL1 pathway (Iwata et al., 2013). The TGFβ pathway has also been investigated in murine tongue development through disruption of TGFβr1 (ALK5) in CNCC, which leads to severely disrupted tongue muscle formation via a lack of BMP4-mediated myogenic proliferation and FGF4/6-mediated myogenic differentiation (Han et al., 2014). There is also evidence of an important role for canonical WNT signal transduction during tongue development. A loss of WNT secretion from the early tongue epithelium results in tongue hypoplasia, and an absence of intrinsic muscles. This is likely due to a requirement for WNT signalling in the underlying CNCC-derived connective tissue and muscle progenitor cells. Specifically, a WNT-NOTCH-PAX7 pathway is required for muscle progenitor proliferation; whilst NOTCH feeds back to negatively regulate WNT-induced CNCC-derived connective tissue proliferation and differentiation (Zhu et al., 2017).

Sonic hedgehog (SHH) is a secreted signalling protein that plays a key role in many diverse biological events extending from early development through to post-natal tissue homeostasis (Briscoe and Therond, 2013, Ingham and McMahon, 2001, Ingham et al., 2011, McMahon et al., 2003, Castillo-Azofeifa et al., 2018). SHH signals from three key regions of

ectoderm in the early head, which includes the ventral forebrain, frontonasal process and oropharynx (Helms et al., 2008, Marcucio et al., 2011, Petryk et al., 2015, Tapadia et al., 2005, Xavier et al., 2016). Specifically, *Shh* is expressed from E9.5 in the pharyngeal endoderm and oropharyngeal epithelium of the first (mandibular) pharyngeal arch (Firulli et al., 2014, Billmyre and Klingensmith, 2015, Xu et al., 2019) with this expression maintained in the primordial tongue epithelium before localizing to fungiform papillae of the anterior tongue from E12.5 (Jung et al., 1999, Sagai et al., 2009; Supplemental figure 1). The significant function of SHH in taste cells has substantial evidence (Castillo et al., 2014, Miura et al., 2014). Blocking SHH in embryonic rat pharyngeal explant culture arrests development of the early primordium (Liu et al., 2004) and signalling to CNCC appears to be an essential requirement. *Nkx2.5-Cre*; *Shh*$^{flox/flox}$ mice lacking SHH from the early pharyngeal endoderm and oropharyngeal epithelium have aglossia and micrognathia (Billmyre and Klingensmith, 2015; Moses et al., 2001); as do *Wnt1-Cre*; *Smo*$^{n/c}$ (Jeong et al., 2004; Xu et al., 2019) and *Wnt1-Cre; Kif3*$^{flox/flox}$ mice (Millington et al., 2017), which lack SHH responsiveness in CNCC from their point of migration through abrogated function of the essential Smoothened (SMO) transducer and the primary cilium, respectively. These studies have demonstrated a role for SHH transduction within CNCC during establishment of the early tongue primordium, although the local contribution of SHH during subsequent development of this organ is less clear.

The conserved long-range *cis*-regulatory enhancers Mammal Fish Conserved Sequence 4 (*MFCS4*) and Mammal Reptile Conserved Sequence 1 (*MRCS1*) located 600-900 Kb upstream of the mouse *Shh* locus drive regional *Shh* expression in the epithelial lining of the oral cavity and pharynx (Sagai et al., 2009). Specifically, *MFCS4* directs *Shh* expression in epithelium of the primordial tongue, pharyngeal and laryngeal areas from E11.0, whilst *MRCS1* regulates expression in the anterior fungiform papillae only from around E12.5.

Targeted deletion of *MFCS4* in mice (*MFCS4*$^{-/-}$) results in severely downregulated *Shh* expression in epithelia of the pharyngeal and laryngeal regions, leading to truncation of the soft palate, slight deformation of the tongue, loss or reduced size of the epiglottis and hypotrophy of the arytenoid accompanied by hypoplasia of multiple laryngeal cartilaginous elements (Sagai et al., 2009). However, some Hedgehog signalling activity does remain in anterior regions, of the tongue primordium in these mice, consistent with the predominantly posterior pharyngeal and laryngeal phenotype, and suggestive of a requirement for SHH signalling in tongue development after establishment of the early primordium.

In this study, we have utilized a series of genetic approaches to investigate the temporospatial contribution of SHH signalling during tongue formation, focusing on timing and the local effect on tissues responding to this pathway within the oral cavity. We find that production of SHH ligand in tongue epithelium from E10.5-12.5 is crucial for lingual tendon formation and a prerequisite for normal patterning of the intrinsic musculature, occurring primarily through local signalling to CNCC within the tongue primordium. Moreover, we provide further insight into the tongue phenotypes seen in patients with disrupted Hedgehog signalling, including the ciliopathies, where the relative contribution of local signalling interactions and global timing of developmental events during tongue development is unclear.

RESULTS

SHH in the oropharyngeal epithelium is required for intrinsic muscle organization in the developing tongue

To explore the function of SHH signalling within the tongue primordium, we first studied *Shh*$^{MFCS4/-}$ mutant mice where one allele lacks *MFCS4*, a key cis-enhancer element for *Shh* expression in tongue epithelium activated at E11.0 (Sagai et al., 2009) and *Shh* is

conventionally deleted in the other allele. It was predicted that an almost complete loss of *Shh* would occur in tongue and pharyngeal epithelia of the mouse, whilst the remaining tissues would be heterozygous for *Shh* expression. We confirmed that in comparison to WT littermates, SHH signalling was significantly decreased in the developing tongue of $Shh^{MFCS4/-}$ mice by E11.5, as demonstrated by reduced *Shh* and *Patched-1* (*Ptch1*) expression (Figure 1A-D) and consistent with the known period of *MFCS4* activity (Sagai et al., 2009). In addition, we also observed slightly decreased *Gli1* expression in the mutant (Figure 1E and F) (Millington et al., 2017). At this stage of development, *Myf5*-positive occipital somite-derived myoblasts have reached the developing tongue primordia in both WT and $Shh^{MFCS4/-}$ mice (Figure 1G and H), confirming that myoblast migration into the tongue primordium was not affected in these mice and in contrast to mice with disrupted SHH signalling in CNCC through loss of primary cilia (Millington et al., 2017). The presence of myoblast differentiation was also confirmed in WT tongue through the detection of *Myod1* and desmin in anterior and posterior regions at E11.5 (Figure 1Ia-Lp). Interestingly, myoblasts present anteriorly expressed *Myod1* but not desmin at this stage (Figure 1Ia and Ka), whilst those more posteriorly located expressed both markers (Figure 1Ip and Kp). Desmin is a marker of more advanced myoblast differentiation than *Myod1*, thus myoblast differentiation progresses from posterior to anterior during normal tongue development. The expression pattern of *Myod1* and desmin was not altered in $Shh^{MFCS4/-}$ mutants (Figure 1Ja and Jp; La and Lp). At E12.5, analysis confirmed the decrease in SHH signalling whilst myogenic differentiation was not affected (data not shown). These observations were confirmed by quantitative RT-PCR (Figure 1M).

At E13.5, the establishment of myotube organization in both intrinsic and extrinsic muscles was indicated by the expression pattern of *Myod1* and desmin in WT (Figure 1N and P). In $Shh^{MFCS4/-}$ mice, this arrangement was disrupted and distinct in the superior (sl) and

174 inferior longitudinal (il), vertical (v) and transverse intrinsic (ti) muscles; whilst in lateral
175 regions where the bilateral extrinsic styloglossus (sg) muscles run, there was no significant
176 disruption (Figure 1O and Q). All *Shh*$^{MFCS4/-}$ mutants died between P0-0.5 with cleft palate,
177 and at this stage the mutant also exhibited disorganised intrinsic muscle fibres based upon
178 SMA IHC (Figure 1R-U). Interestingly, the disorganized intrinsic muscle arrangement was
179 rarely found in the tongues of *MFCS4* homozygous-deleted mice (*Shh*$^{MFCS4/MFCS4}$)
180 (Supplemental figure 2).

181 The cleft palate observed in *Shh*$^{MFCS4/-}$ animals was caused by a failure of palatal shelf
182 elevation, which requires intrinsic elevation forces within the shelves and extrinsic factors,
183 such as clearing of the tongue from the roof of the mouth due to involuntary and swallowing
184 movements. Maxillary organ culture showed that although the soft palate was shorter in an
185 anterior-posterior direction, the palatal shelves of *Shh*$^{MFCS4/-}$ fetuses successfully elevated and
186 were able to fuse in the midline (Supplemental figure 3). Combined with previous studies on
187 tongue obstruction leading to cleft palate (Tsunekawa et al., 2005; Iseki et al., 2007), we
188 hypothesized that decreased SHH signalling in the tongue results in disorganized intrinsic
189 muscle arrangement, which leads to cleft palate. This idea was supported by the observation
190 that the penetrance of cleft palate was limited in *Shh*$^{MFCS4/MFCS4}$ (13.5 per cent in Sagai et al.,
191 2009 versus 100 per cent in *Shh*$^{MFCS4/-}$).

192 The finding of some residual *Shh* expression in the *Shh*$^{MFCS4/-}$ tongue after the
193 *MFCS4*-activated stage (E11.0) suggested the presence of other factors regulating *Shh*
194 expression in this region. Thus, use of the *Shh*$^{MFCS4/-}$ mutant in this study allowed us to
195 examine the consequences of severely decreased epithelial *Shh* expression combined with a
196 decrease of SHH signalling within the tongue primordium.

197

198 **SHH from the tongue epithelium is required for lingual tendon formation**

CNCC within the developing tongue have been suggested to act as a scaffold during the organization of lingual myoblasts and myotubes (Parada et al., 2012). Patterning of the tongue musculature occurs simultaneously with tendon development and includes formation of the *aponeurosis linguae* and lingual septum within the tongue dorsum as flat broad transverse and vertical sheathes of midline fibrous tissue, respectively. We investigated expression of the tenocyte marker *Scleraxis* (*Scx*) (Schweitzer et al., 2001) using ISH and found low-level expression from E11.5 in posterior regions of the tongue, but not the anterior (Figure 2A and data not shown), consistent with the pattern of muscle localization in the WT. At E12.5, an M-shaped expression domain was seen (Figure 2C), coinciding with the expression pattern seen in whole mount (Figure 2E). In contrast, there was little evidence of *Scx* transcripts in $Shh^{MFCS4/-}$ mice at E11.5 (Figure 2B) and only faint expression at E12.5 (Figure 2D), which was confirmed in whole mount (Figure 2F). In addition to expression in the midline at the developing lingual septum (Figure 2G, double-sided arrow), a thin layer of bilateral widespread low-level expression was also found in the tongue dorsum at E13.5 in the WT, indicating aponeurosis linguae formation for the intrinsic muscles (Figure 2G, dotted line). Outside of the tongue, there was strong bilateral expression of *Scx* at sites of tendon formation associated with the paired extrinsic genioglossus muscles (Figure 2G, arrowheads). In contrast, $Shh^{MFCS4/-}$ mice failed to develop *Scx*-positive tendons for the intrinsic muscles at E13.5 (Figure 2H), despite clear expression in the extrinsic genioglossus muscle tendons (Figure 2H, arrowheads). Expression of *Scx* in the tongue dorsum was significantly decreased; however, low levels of *Scx* expression in the lateral regions was occasionally observed in the mutant (Figure 2F and H, arrows). Since *Shh* expression and *MFCS4* activation were found in the dorsal lingual epithelium, these observations suggested involvement of other factors in tenocyte differentiation on the lateral sides of the tongue. Detection of CD31 and synaptophysin, markers for vascularization and innervation

respectively, did not indicate any particular differences between WT and *Shh*$^{MFCS4/-}$ mice at E13.5 (Supplemental figure 4).

CNCC-derived differentiation but not proliferation is affected in the tongue of *Shh*$^{MFCS4/-}$ mice

We further analysed CNCC differentiation in *Shh*$^{MFCS4/-}$ mice through the expression of *Sox9*, a marker for CNCC as well as a common representative transcription factor for chondrocyte, ligament cell and tenocyte differentiation (Mori-Akiyama et al., 2003, Spokony et al., 2002). *Sox9* expression was transiently evident during the early stages of tongue development in the WT, with strong expression established in the future lingual septum-forming region by E12.5 (Figure 2I arrow); however, by E13.5 *Sox9* expression had dissipated in the WT and replaced by *Scx* marking the lingual septum (data not shown). In contrast, *Sox9* was only weakly expressed at E12.5 in the mutant (Figure 2J). Collectively, these data suggest that in the process of tenocyte differentiation from CNCC-derived tongue primordium mesenchyme there is a transition stage, during which WT mesenchyme expresses both *Sox9* and *Scx*, whereas in the mutant there was a failure to properly express either gene.

In accordance with the *Scx* expression pattern, *type I collagen* (*Col1a1*) and *fibronectin* (*Fn1*), which mark the extracellular matrices of tendon tissues were clearly transcribed in WT tendon, including the aponeurosis and septum (Figure 2K and M); whereas their expression in the *Shh*$^{MFCS4/-}$ tongue was weak and not well patterned (Figure 2L and N). We next studied cell proliferation in the tongue mesenchyme at E11.5 and 12.5 during which, tenocyte specification occurs in CNCC. However, there were no significant differences in proliferative activity of CNCC-derived mesenchyme or myoblasts during this period (Figure 2O) and no differences in patterns of cell death (assayed through active caspase-3 detection, data not shown) in WT or mutant embryos.

SHH is required for appropriate arrangement of the intrinsic musculature after tongue primordium formation

The analysis of *Shh*$^{MFCS4/-}$ mutant mice demonstrated an essential role for SHH signalling in the tongue primordium; however, *Shh* expression continues in the oropharyngeal epithelium before early tongue primordium formation and until a prototype intrinsic lingual muscle arrangement is established (see Supplemental figure 1) (Sagai et al. 2009). Furthermore, some SHH activity is still present in *Shh*$^{MFCS4/-}$ embryos, mediated through *Shh* transcription independent of *MFCS4* activity (Figure 1B, D, F). Therefore, we investigated the temporal requirements of SHH during tongue formation using stage-specific abrogation of gene function. Specifically, we crossed *pCag-CreER*^{TM} mice (Hayashi and McMahon, 2002) with a line harbouring a conditional (floxed) *Shh*^{c} allele (Dassule et al., 2000). Single maternal tamoxifen administration was carried out at E10.5, 11.5 and 12.5, respectively with the tongue phenotype analysed at E14.5. In comparison to WT littermates (Figure 3A and E), significant disorganization of the intrinsic musculature was present within the tongue, which was grossly dependent upon timing of signal loss (Figure 3B-D, F-H). In mice treated with tamoxifen at E10.5, in comparison to WT the normal striated architecture of the intrinsic muscles was lost and tongue size reduced (Figure 3A and E; B and F), whilst deletion at later stages resulted in progressively less severe disruption of myogenic pattern (Figure 3C and G; D and H; Supplemental figure 5). mRNA ISH for *Myod1* suggested that myoblast differentiation had occurred in both the intrinsic and extrinsic musculature, even in the most severely affected mutants (E10.5 treatment, Figure 3J), but that organization of the myotubes was defective (Figure 3I-L). In comparison to the WT, *Scx* expression was lost in the midline septum and significantly down-regulated in aponeurosis-forming regions of the dorsum, whilst expression remained in the developing genioglossus and geniohyoid tendons of the

mutant (Figure 3M and N). *Scx* expression in the midline dorsum was progressively increased in fetuses exposed to the later injections (at E11.5 and 12.5, Figure 3O and P). Collectively, these data demonstrate an important timing-dependent role for SHH signalling after E10.5 in mediating normal tendon architecture and organization of the intrinsic musculature of the tongue, with low levels of SHH signalling present in $Shh^{MFCS4/-}$ mice sufficient to support gross growth of the tongue. Interestingly, examination of K14-*Shh* transgenic embryos, which over-express *Shh* in the developing tongue epithelium from around E11.5 (Cobourne et al., 2009) revealed a gross distortion of tongue architecture at E15.5 but a seemingly normal arrangement of the intrinsic muscles within the body of the tongue (data not shown). Therefore, myoblast organization and differentiation is able to occur in the presence of excess SHH signal from the tongue epithelium during development.

SHH signalling in the developing tongue targets CNCC through the primary cilium

Given that myoblast migration and differentiation was not seemingly affected by decreased SHH signalling in the tongue after E11.0, but that tendon formation and myotube arrangement specifically were, we hypothesized that CNCC were the direct recipients of SHH signals. We therefore investigated the spatial relationship between SHH responding cells, CNCC and myoblasts in the developing tongue (Figure 4A-E). Specifically, we examined the tongue of *Wnt1-Cre; R26R* embryos, which constitutively express beta-galactosidase in CNCC (and their progeny) from their point of exit at the neural tube (Chai et al., 2000). At E12.5, X-gal staining for beta-galactosidase revealed the distribution of CNCC in the developing tongue (Figure 1A-C); whilst mRNA ISH for *Ptch1* on adjacent sections indicated that CNCC-derived mesenchymal cells expressed *Ptch1* and were therefore a primary target of SHH signal transduction during tendon formation and myotube arrangement (Figure 4D). In contrast, *Myf5* was expressed in a broadly complementary pattern, suggesting

that mesodermal cells are not the direct target of SHH in the tongue (Figure 4E). Interestingly, mRNA ISH of *Gli1* showed a more uniform expression within the tongue, whilst the SHH co-receptor-encoding genes *Gas1*, *Cdo* and *Boc* were detected in the mesenchymal core including myoblasts and more peripheral regions in domains consistent with a negative correlation between co-receptor expression and SHH signal levels (Martinelli and Fan, 2007) (Supplemental figure 6).

SHH ligand binds to the Ptch1 receptor at the primary cilium of receiving cells, with the cilium recognized as a key cellular organelle necessary for normal Hedgehog signal transduction (Huangfu and Anderson, 2005). Consistent with this, human patients with ciliopathic loss-of-function OroFacioDigital 1 (*OFD1*) mutations have multiple craniofacial anomalies, including cleft palate and tongue defects that involve clefting, cystic formation and hamartoma (Fenton and Watt-Smith, 1985). Animal models of *Ofd1* also lead to a ciliogenesis defect and loss of SHH signal reception (Adel Al-Lami et al., 2016, Ferrante et al., 2006) and mice lacking function of the Kif3a ciliary protein in CNCC have aglossia (Millington et al., 2017). We generated CNCC-specific deletion in *Ofd1* using *Wnt1-Cre; Ofd*$^{fl/Y}$ mice and found decreased levels of *Ptch1* expression in CNCC-derived mesenchyme at E11.5 and 12.5 (Figure 4F, G, I, J). In contrast, *Mesp1-Cre; Ofd*$^{fl/Y}$ embryos, which have *Ofd1* deletion in mesodermal cells from the onset of gastrulation (Saga et al., 1999) had relatively normal levels of *Ptch1* expression in the tongue (Figure 4H and K). Significantly, there was a complete loss of normal myotube arrangement and hypoglossia in *Wnt1-Cre; Ofd*$^{fl/Y}$ embryos (Figure 4L and M); whilst in *Mesp1-Cre; Ofd*$^{fl/Y}$ mutants, myotube arrangement was largely unaffected (Figure 4N). These observations further suggested that muscle patterning of the tongue requires SHH signalling from the epithelium to CNCC after tongue primordium establishment.

TGFβ and FGF signalling are influenced by Shh in the developing tongue

TGFβ signalling has previously been shown to mediate interactions between CNCC and myoblasts during cell proliferation, differentiation and tongue muscle organization (Hosokawa et al., 2010, Han et al., 2014) and Tgfβ receptors are transcribed in developing tongue mesenchyme (Hosokawa et al., 2010; Millington et al., 2017), which suggests potential cross-talk between TGFβ and SHH signalling. We therefore examined transcription of the ligands *Tgfb1, -2,* and *-3* at E12.5 in WT and $Shh^{MFCS4/-}$ mice using section ISH (Figure 5A-F). *Tgfb1* did not show any defined expression within tongue mesenchyme of WT mice, but *Tgfb2* was detected in the myoblasts and *Tgfb3* in the lingual septum (Figure 5A, C, E). Whilst *Tgfb1* did not show any expression in $Shh^{MFCS4/-}$ mutants either, *Tgfb2* and *-3* were both down-regulated in the intrinsic musculature (Figure 5B, D, F). However, these changes were subtle and whilst qPCR analysis confirmed this trend, the changes were not significant (Supplemental figure 7). Therefore, we further investigated TGFβ signalling in *pCag-*$CreER^{TM}$*;* $Shh^{flox/flox}$ mice using temporally-controlled deletion of *Shh.* As SMAD2 and -3 are essential components of the TGFβ intracellular signal transduction pathway, their phosphorylation (pSMAD2/3) was examined by Western blotting of the tongue of *pCag-*$CreER^{TM}$*;* $Shh^{flox/flox}$ mice treated with tamoxifen at E10.5 and analysed at E13.5. Interestingly, pSMAD2/3 was significantly reduced in all mutants when compared to controls (Figure 5G). It has also been demonstrated that FGF signalling contributes to tenocyte differentiation in other parts of the body (Brent et al., 2003, Brent et al., 2005, Sukegawa et al., 2000, Du et al., 2016). We found that *Fgfr1* was expressed in the aponeurosis and septum in WT mice; however, *Fgfr1* transcripts were significantly reduced in $Shh^{MFCS4/-}$ mice both by qRT-PCR comparison and by ISH (Figure 5H-J) confirming the potential involvement of FGF signalling in tendon formation. Finally, we also considered the possibility that WNT signalling could also be affected in our mutant models (Zhu et al., 2017). However, neither

RT-PCR analysis of the WNT target gene *Axin2* in *Shh*$^{MFCS4/-}$ mice at E12.5, or mRNA ISH for *Axin2* at E14.5 in *pCag-CreER*^{TM}; *Shh*$^{flox/flox}$ mice treated with tamoxifen at E10.5 showed any significant differences (Supplemental figure 7).

Taken together, these data demonstrate that a loss, or decreased SHH in the developing tongue epithelium from the time of tongue primordium establishment results in disrupted patterning of the lingual tendon and intrinsic tongue musculature, which is potentially mediated through TGFβ and FGF signalling.

DISCUSSION

Tongue anomalies are a common finding amongst the constellation of defects that can affect the developing craniofacial region (Cobourne et al., 2018). Perhaps somewhat surprisingly, the developing tongue has not been investigated to the same extent as other regions of the craniofacial complex. Here, we demonstrate a key role for SHH signalling from epithelium of the developing tongue primordium to CNCC during tendon formation and patterning of intrinsic musculature within the mammalian tongue. These findings are consistent with the commonly observed tongue defects seen in the ciliopathies, arising through defective SHH transduction within the primary cilium.

A local requirement for SHH signalling to CNCC during formation of the lingual septum and patterning of the intrinsic tongue musculature

A number of molecular signalling pathways have been implicated in tongue formation (Parada et al., 2012) but the temporospatial tissue interactions regulating local organisation of this organ are not fully established. *Shh* is expressed in multiple regions of the early pharyngeal epithelium and global disruption of signalling prior to formation of the tongue anlage ultimately leads to aglossia (Billmyre and Klingensmith, 2015). SHH signalling to

CNCC migrating through this region is clearly essential for this process, as mice engineered with loss of Hedgehog responsiveness in this population have aglossia (Jeong et al., 2004; Millington et al., 2017; Xu et al., 2019). However, local *Shh* expression is maintained in epithelium of the early tongue primordium, but the significance of this signalling is unclear. Indeed, it has recently been demonstrated that Hedgehog signalling to CNCC is required for appropriate specification of the oral mandibular mesenchyme, with loss of *Smo* function in early post-migratory CNCC within this region associated with aglossia and ectopic bone formation in the oral mandibular mesenchyme. Specifically, *Hand2-Cre; Smo*$^{c/c}$ embryos lacking *Smo* function in the mandibular arch from around E9.5 display a tongue that is rudimentary and associated with significantly reduced numbers of *Myf5*-expressing muscle precursor cells (Xu et al., 2019). Interestingly, *Gas1*$^{-/-}$*; Boc*$^{-/-}$ mice with reduced Hedgehog signalling activity secondary to loss of essential SHH co-receptor function have cleft of the pharyngeal tongue as part of their constellation of midline craniofacial defects (Seppala et al., 2014).

Here, we show that timing of SHH loss from E10.5 causes disruption to the intrinsic musculature with small size, but not aglossia; demonstrating an essential temporal role for local SHH signalling in tongue formation and consistent with the known expression domain (Figure 6A, D). We also demonstrate that SHH directly induces formation of the CNCC-derived lingual septum, which are required for normal myotube arrangement within the intrinsic musculature. The crucial time-point for this requirement appears to be from E11.0, as expression of *Shh* in the epithelium via the *MFCS4* enhancer is important for this process and removal of the enhancer activity from one allele and *Shh* expression from the other allele theoretically resulting in severely decreased SHH signaling in CNCC-derived mesenchyme from E11.0 was associated with defective tendon formation. Collectively, these results suggest that SHH from the oropharyngeal epithelium is required to induce tongue

399 primordium formation before E10.5 and subsequent signalling from the oropharyngeal and
400 early primordial tongue epithelium is required for the differentiation of lingual tendons
401 during intrinsic tongue muscle patterning (Figure 6F). Although *Shh*$^{MFCS4/-}$ mice could have a
402 complete loss of *Shh* in the tongue epithelium from E11.0 onwards, it is conceivable that
403 residual SHH signalling activity remains. Indeed, we found that expression of *Shh* and *Ptch1*
404 were not completely lost in these mice (see Figure 1A-D). Similarly, complete loss of *Scx*
405 expression also did not always occur. One possibility is that additional *Shh* enhancers or
406 regulatory factors can compensate for loss of *MFCS4* function; however, the other known
407 oropharyngeal epithelium enhancer *MRCS1* is unlikely to be responsible, as it only activates
408 *Shh* expression after E12.5 (Sagai et al., 2009) when expression of *Scx* has already been
409 initiated in the tendon-forming area. Therefore, the precise regulatory mechanisms
410 underlying *Shh* expression in the oropharyngeal epithelium during tongue formation remains
411 to be fully elucidated (Irimia et al., 2012; Anderson and Hill, 2014). Since we observed
412 slightly small tongue size when tamoxifen was treated on E11.5 *pCag-CreER*^{TM}; *Shh*$^{flox/flox}$
413 mice, the remaining SHH signal in the *Shh*$^{MFCS4/-}$ functions in tongue size growth, which is
414 supported by the observed cell proliferation within the tongue primordium (Fig. 2O).
415
416 **SHH signalling and tendon formation**
417 The contribution of SHH signalling in tendon formation has been reported in a variety of
418 anatomical systems, including the trunk, limb and head (Schweitzer et al., 2001, Subramanian
419 and Schilling, 2015) but not the tongue. In all these systems, tendons are specialized
420 connective tissues that assemble musculoskeletal tissues and anchor force-generating muscles
421 to the skeleton, which leads to optimal locomotion and mobility in vertebrates. Consistent
422 with our findings, a common feature of early tendon formation is the relationship between
423 SHH and FGF signalling. During chick axis tendon formation, *Shh* expressed from ventral

midline structures such as the floor plate and notochord inhibits induction of syndetome, which is comprised of tendon progenitor cells. However, SHH indirectly induces *Scx* expression through activation of FGF in the dermomyotome, which promotes *Scx* transcription in the somite (Brent et al., 2003). In support of this, FGF signalling is required for differentiation of tenocyte precursors in mice (Brent et al., 2005). In the chick digestive system, expression of *Scx* in two tendon domains that develop in close relation to the two visceral smooth muscles also depends upon FGF signalling (Le Guen et al., 2009) and *Shh* expressed from the endoderm is involved in regulation of smooth muscle cell and tenocyte differentiation (Sukegawa et al., 2000). A recent study has reported that expression levels of some FGFs are increased during the period of lingual septum formation (Du et al., 2016), which suggests the involvement of FGF signalling in lingual tenocyte differentiation. In support of this, we detected diminished expression of *Fgfr1* in the lamina propria, future aponeurosis and lingual septum of the $Shh^{MFCS4/-}$ tongue. Thus, we suggest that the differentiation of tenocytes derived from CNCC is positively regulated by SHH signalling via FGF's.

CNCC function, myogenic precursor cells and development of the tongue

Several previous studies have indicated that normal CNCC function is required for the initiation of tongue formation through SHH signalling (Jeong et al., 2004; Millington et al., 2017; Xu et al., 2019). These investigations have shown that disrupting Hedgehog responsiveness in CNCC from their point of migration results in large-scale apoptosis of these cells within the first arch, an accompanying failure of mesoderm-derived muscle precursor cell migration into the tongue anlage leading to aglossia (Jeong et al., 2004; Millington et al., 2017). However, the role of SHH during regulation of subsequent developmental events, such as myoblast differentiation is less clear. *Pax3*-positive muscle

progenitors begin migration at E9.75 and reach the pharyngeal region subsequent to CNCC populations by around E11.5 (Relaix et al., 2004; Han et al., 2012). There are hints from studies of TGFβ signalling during murine tongue formation of a complex interplay between CNCC and myogenic precursor cells (Han et al., 2012, Hosokawa et al., 2010). Our data points to a key step in tongue development whereby CNCC receive epithelial SHH cues in the tongue primordium, which are essential for the normal organization of intrinsic myogenic precursors, but not for myoblast differentiation. However, the expression of *Shh* and its related molecules (Supplemental figure 6) suggests involvement in muscle formation, which requires further investigation.

Molecular targets of SHH signalling in the embryonic tongue

We considered a number of molecular pathways known to regulate early tongue formation that may act downstream of SHH, including TGFβ and WNT signalling. Interestingly, a lack of TGFβ signalling in CNCC has also been shown to affect both tendon and myotube formation (Hosokawa et al., 2010) and there is also evidence that *Scx* expression in the early tongue is dependent upon TGFβ signalling in CNCC, but not in myogenic precursors (Han et al., 2014, Han et al., 2012). However, we found no significant change in *Tgfb2* and *-3* expression. Interestingly, non-significant changes in Tgfb receptor -1 and -2 have previously been reported in *Wnt1-Cre; Kif3a*$^{flox/flox}$ mice (Millington et al., 2017). A change in pSMAD2/3 was detected through Western blot in the tongues of *pCag-CreER*^{TM}*; Shh*$^{flox/flox}$ embryos, which might conceivably be due to potential changes in BMP signalling rather than TGFβ. Indeed, Hedgehog-SMO-GLI1 is required for transcription of the Forkhead box genes *Foxf1*, *Foxf2*; *Foxd1*, *Foxd2* in CNCC (Jeong et al., 2004; Millington et al., 2017; Everson et al., 2017) and negatively regulates BMP signalling in CNCC through *Foxf1* and *Foxf2* during early patterning and survival of this cell population in the mandibular arch (Xu et al., 2019).

Finally, a loss of WNT secretion from *Shh*-expressing epithelial cells also results in tongue hypoplasia through disrupted development of the epidermis, tenocytes and internal musculature (Zhu et al., 2017). However, we did not observe altered *Axin2* expression in $Shh^{MFCS4/-}$ or $pCag\text{-}CreER^{TM}; Shh^{flox/flox}$ mice. Therefore, whilst changes in pSMAD2/3 were detected following loss of SHH signalling from the tongue epithelium, WNT signalling appears not to be involved in the mutants used in this study. The association between TGFβ, BMP, WNT and SHH signalling at different stages of development within the mandibular arch is not clear and further work will be required for these complex interactions to be elucidated.

Tongue defects in the ciliopathies through disrupted Hedgehog signalling

As our hypothesis was that CNCC are key recipients of the SHH signal within the developing tongue, we considered models of human OFD1 that are predicted to be neurocristopathies. OFD1 patients have a spectrum of craniofacial phenotypes including gingival frenulae, lingual hamartomas, cleft palate and significantly, cleft and/or lobulated tongue (Franco and Thauvin-Robinet, 2016). Moreover, ablation of the Kif3a ciliary protein in CNCC is associated with aglossia (Millington et al., 2017). *Wnt1-Cre;* $Ofd^{fl/Y}$ embryos lacking *Ofd1* function in CNCC had a severely hypoplastic tongue and complete disruption of myotube arrangement. The *Ofd1* gene is located on the X-chromosome and encodes a component of the centrosome and basal body of primary cilia, a key mediator of SHH signalling (Satir et al., 2010). Impaired function of the cilium results in a variable effect on signal transduction, affecting not only SHH but also other pathways such as WNT, depending upon the molecular context (Bangs et al., 2015). Again, while further investigation is required to clarify the cross-network interactions between SHH, FGF, TGFβ, BMP and WNT signalling during tongue formation, we note that the majority of phenotypes can be attributed to *Shh* expression

from the epithelium. It is of further note that in contrast to *Wnt1-Cre; Kif3a*$^{flox/flox}$ embryos (Millington et al., 2017), *Wnt1-Cre; Ofd*$^{fl/Y}$ embryos did not show aglossia but hypoglossia, which is suggestive that SHH signals can be transduced to some extent in these mice, which may be a useful tool for further analysis of SHH signalling in orofacial development.

Taken together, investigation of these temporospatial tissue-tissue interactions provides new insight into formation of the tongue, specifically the tendons and intrinsic musculature and reveal how localised signalling can influence gross structure and function of this highly adapted organ.

Materials and methods

Animals

All animal experiments were approved by the Institutional Animal Care and Use Committees of Tokyo Medical and Dental University (0170238A), King's College London (PPL7007441 and PPL P8D5E2773, KJL), and National Institute of Genetics (28-7). *MFCS4*$^{+/-}$ (RRID: MGI:6144004, Sagai et al., 2009), *Shh*$^{-/+}$ (RRID: MGI:6144003, Amano et al., 2009), *pCag-CreER*^{TM} (RRID: IMSR_JAX:017595, Hayashi and McMahon, 2002), *Shh*$^{flox/+}$ (RRID: MGI:3580473, Dassule et al., 2000), *Wnt1-Cre* (Danielian et al., 1997), *Mesp1-Cre* (RRID: IMSR_RBRC01145, Saga et al., 1999) and *ROSA26* reporter (*R26R*) (Soriano, 1999) mice were maintained in a C57BL/6N background, whilst *Ofd*$^{fl/Y}$ (Ferrante et al., 2006) were maintained in a CD-1 background. In compound heterozygote *Shh*$^{-/+}$*; MFCS4*$^{+/-}$ mice (here referred to as *Shh*$^{MFCS4/-}$) the (*MFCS4*) long-distance *Shh* enhancer is deleted on one allele, whilst the (*Shh*) gene remains intact on the same allele. *pCag-CreER*^{TM}*; Shh*$^{flox/+}$ mice were mated with *Shh*$^{flox/+}$ mice, with pregnant mice receiving tamoxifen by intraperitoneal injection (75 mg/kg, equivalent to 3 mg per 40g body weight) through the maternal body at

the appropriate developmental stage. All comparisons were performed between the mutants above versus wild type (WT) littermates.

Histological analysis

Specimens were fixed with Bouin's solution for Haematoxylin and Eosin (H+E) staining or fixed in 4% paraformaldehyde (PFA) in PBS for embedding in paraffin or OCT compound (Sakura Finetek, Tokyo, Japan) for other histological analyses. Sections were taken at 5 micron- (paraffin) or 12 micron-thick (frozen) sections. All paired images for comparison were derived from littermates and representative of at least 3 independent experiments.

Immunohistochemistry

For immunohistochemistry (IHC), anti-desmin antibody (clone D33, 413651, Nichirei Biosciences, Tokyo, JP) at 1:1 dilution, anti-smooth muscle actin (SMA) antibody (RRID: AB_476701, clone 1A4, A2547-100UL, Sigma, Saint Louis, MO) at 1:1000 dilution, anti-Bromodeoxyuridine (BrdU) antibody (clone BMC9318, 11 170 376 001, Roche Diagnostics, Basel, CH) at 1:100 dilution, anti-MYF5 antibody (RRID: AB_10744494, polyclonal, SAB4501943, Sigma) at 1:100 dilution, anti-CD31 antibody (RRID: AB_726362, polyclonal, ab28364, Abcam, Cambridge, UK) at 1:100 dilution, and anti-synaptophysin antibody (RRID: AB_2198854, clone SY38, ab8049, Abcam) at 1:100 dilution were used. For visualization, corresponding secondary antibodies, Vectastain ABC Kit (RRID: RRID:AB_2336827, AK-5000, Vectastain, Burlingame, CA) and diaminobenzidine (DAB) were applied, or corresponding fluorescent-conjugated secondary antibody was applied. Hematoxylin to counterstain DAB labeled sections and Hoechst 33342 was used to stain DNA in fluorescent sections.

549 ***In situ* hybridization**

550 For *in situ* hybridization (ISH) specimens were hybridized in whole mount or section using
551 digoxygenin-labeled RNA probes specifically designed complementary to the partial-mRNA
552 of *Shh*, *Ptch1*, *Gli1*, *Myf5*, *Myod1*, *Sox9*, *Scx*, *ColIa1*, *Fn1*, *Fgfr1*, *Ptch2*, *Cdon*, *Boc*, *Gas1*,
553 *Hhip*, *Tgfb1*, *-2*, and *-3*, and *Axin2*, followed by incubation with anti-digoxygenin-AP
554 conjugate. Nitro blue tetrazolium chloride (NBT)/5-Bromo-4-chloro-3-indolyl phosphate,
555 toluidine salt (BCIP) were used for visualization. Section ^{35}S (PerkinElmer, Beaconsfield,
556 UK) radioactive ISH was carried out for *Shh* and *Ptch1* as previously described (Cobourne et
557 al., 2004). Light and dark-field images of sections were photographed using a Zeiss Axioskop
558 microscope and merged in Adobe Photoshop CS6. All commercial reagents for ISH were
559 purchased from Roche Diagnostics (Basel, CH). Sequences of the probes were listed in Table
560 1.
561
562 **Beta-galactosidase staining**
563 For the detection of beta-galactosidase activity using X-gal staining, sections were incubated
564 with 5-bromo-4-chloro-3-indolyl-β-D-galactoside (X-gal) in phosphate buffer (pH 7.3)
565 supplemented with 2 mM $MgCl_2$, 5mM potassium ferrocyanide ($K_4Fe(CN)_6$-$3H_2O$), and
566 5mM potassium ferricyanide ($K_3Fe(CN)_6$) at 30°C after fixation in 4% PFA. Nuclear Fast
567 Red was used for counter staining.
568
569 **Organ culture**
570 The dissected maxilla (with vertically oriented palatal shelves) of E13.5 $Shh^{MFCS4/-}$ or WT
571 littermates were cultured in Dulbecco's Modified Eagle's Medium Nutrient Mixture F-12
572 (Sigma) and BGJb Medium (LifeTechnologies, Grand Island, NY) for 48 hours by
573 continuous supply of 95% O_2 + 5% CO_2 at 37°C using a rotary culture system.

574

575 **Cell proliferation analysis**

576 Sixty minutes before dissection, BrdU at 100mg/ml was injected intraperitoneally into
577 pregnant females at 10mg/kg on the designated day. Every 6 of 7 sections through the tongue
578 primordium of a specimen were used for the cellular proliferation analysis. BrdU
579 incorporation and MYF5 localization were detected by IHC. External cells scored as
580 epithelial cells were confirmed by basement membrane staining. Myoblast cell lineage was
581 determined as MYF5-positive cells, and MYF5-negative cells were considered to be CNCC-
582 derived. A proliferation index was calculated from the number of BrdU-positive cells divided
583 by the total number of cells of each population and statistical significance was examined by
584 Student *t*-test for more than 3 individual experiments for each genotype.

585

586 **Real time RT-PCR**

587 RNA was extracted from the tongues of $Shh^{MFCS4/-}$ and WT littermate embryos at E12.5 using
588 Direct-zol RNA MiniPrep Kit (R2050S, Zymo Research, Irvine, CA) following the product
589 protocol. 250 ng mRNA was transcribed to cDNA by ReverTra Ace (TRT-101, Toyobo Life
590 Science, JP). Realtime PCR was performed with LightCycler 480 High Resolution Melting
591 Master (04909631001, Roche Diagnostics). The expression was normalized to the *actin, beta*
592 gene and relative expression to the littermate WT was shown. Statistical significance was
593 examined by *t*-test for more than 3 individual experiments for each genotype. The primer
594 sequences are listed in Table 2.

595

596 **Western blotting**

597 Whole tongue lysates were obtained from $pCag\text{-}CreER^{TM}$; $Shh^{flox/flox}$ and WT littermate
598 embryos in radioimmunoprecipitation assay (RIPA) buffer (ThermoFisher Scientific,

599 Waltham, MA) (n=3 for each). Equivalent amounts of protein lysate were run on a 4-12%
600 gradient Norex gel (ThermoFisher Scientific, Waltham, MA) and separated proteins
601 electro-transferred onto a nitrocellulose membrane. Phosphorylated SMAD2/3
602 (pSMAD2/3) and beta actin (β-actin) were detected using the corresponding antibodies
603 (Phospho-SMAD2 (Ser 465/467) / SMAD3 (Ser 423/425) (D27F4) Rabbit monoclonal
604 antibody; Beta actin (13E5) Rabbit monoclonal antibody) (RRID: AB_2631089 and
605 AB_10694076, Cell Signalling Technology, Danvers, MA) both at 1:1000 dilution. Bands
606 were analysed using the Chemidoc MP imaging system (Bio-Rad laboratories,
607 Hercules, CA) and intensity was measured using Image lab software
608 (RRID:SCR_014210, version 5.2.1). Band intensities were normalized against β-actin
609 and data plotted on a histogram. The integrated volume of pSMAD2 and 3 bands were
610 divided by that of β-actin band and statistically examined for comparison.
611

612 **Table 1 Probe sequences**

613 Molecular riboprobes used in this study.

probes used in this study (in order of appearance)

gene symbol	NCBI accession	span	length (base)	GC (%)	note
Shh	NM_009170.3	455..1097	643	57.2	
Ptch1	NM_008957.3	631..1442	812	48.2	
Gli1	NM_010296.2	1162..2589	1428	61.7	*
Myf5	NM_008656.5	810..1962	1153	32.6	
Myod1	NM_010866.2	781..1754	974	56.8	
Scx	NM_198885.3	705..1103	399	52.9	
Sox9	NM_011448.4	2842..3142	301	52.2	
Col1a1	NM_007742.4	2670..3314	645	65.3	
Fn1	NM_010233.2	6444..7211	768	53.3	
Ptch2	NM_008958.3	862..1670	809	62.3	
Hhip	NM_020259.4	497..1106	610	52.3	

Gas1	NM_008086.2	1777..2309	533	51.0	
Cdon	NM_021339.2	6573..7043	471	60.0	
Boc	NM_172506.2	444..1243	800	56.4	
Tgfb1	NM_011577.2	1018..1738	721	57.0	
Tgfb2	NM_009367.4	1787..2487	701	47.8	
Tgfb3	NM_009368.3	1336..1945	610	52.5	
Fgfr1	NM_010206.3	703..3228	2526	56.1	*
Axin2	NM_015732.4	2793..4062	1270	53.1	*

All were subcloned into pTA2 (TAK-101, Toyobo Life Science, Tokyo, JP)

* ; alkaline hydrolysis was performed to have 250bp length in average

Table 2 Primer sequences

Primer sequences for semi-quantitative RT-PCR in Figure 1 and Supplemental figure 7.

Primers for semi-quantitative RT-PCR in Figure 1 and Supplemental figure 7 (in order of appearance)

gene symbol	NCBI accession	primers	span	product length (base)	product GC (%)	note
Shh	NM_009170.3	CAGCTCACAAGTCCTCAGGT	307..441	135	63.7	
		GCCTCTTTCCAAACCCCCTG				
Ptch1	NM_008957.3	TGCACCAAGTGGACACTCTC	2352..2487	136	52.2	targeting transcription variant 1, 2, and X1-5
		TCACTCGGGTGGTCCCATAA				
Gli1	NM_010296.2	CCGACGGAGGTCTCTTTGTC	13..166	154	57.1	
		AACATGGCGTCTCAGGGAAG				
Myf5	NM_008656.5	CGGATCACGTCTACAGAGCC	840..996	157	57.3	targeting transcription variant 1 and X1
		GCAGGAGTGATCATCGGGAG				
Fgfr1	NM_010206.3	GGAGTTAATACCACCGACAAG	1702..1970	269	52.4	targeting transcription variant 1-3, and X1-5
		TTGGTGCCGCTCTTCATCTT				
Tgfb1	NM_011577.2	GCTGCGCTTGCAGAGATTAAA	1329..1486	158	50.0	
		ACTGCCGTACAACTCCAGTG				
Tgfb2	NM_009367.4	CCCCGGAGGTGATTTCCATC	1406..1547	142	59.2	targeting transcription variant 1,2, and X2
		TGGGACGGCATGTCGATTTT				
Tgfb3	NM_009368.3	AGGCTTCCTTCTGGAACATTT	2478..2631	154	48.7	
		TGTCCACTCGCTATCCGTTC				
Axin2	NM_015732.4	ACCTTGCCAAAACGGAATGC	2072..2213	142	62.0	targeting transcription variant 1, and X1-4
		ACATCCACTGCCAGACATCC				

Actb	NM_007393.5	GGGAAATCGTGCGTGACATC GAACCGCTCGTTGCCAATAG	696..844	149	42.3	

617

618

619 ## Acknowledgements

620 This work was supported by JSPS KAKENHI Grant Numbers 19890071, 22592254,
621 25463130 and 16K11744 to SO, and 20390510 to SI, and NIG-JOINT (2008-A, 2009-B7,
622 2012-B4) to SI. HAA is funded by Iraq Higher Committee for Educational Development.
623 KJL received funding from the BBRSC (Grant BB/I021922/1) and MRC (Grant
624 MR/L017237/1). MTC received a Small Research Grant from the Royal College of Surgeons
625 of Edinburgh for generation of transgenic mice. GMX was funded by the programme
626 ALBAN, the European Union programme of high-level scholarships for Latin Americans
627 (E07D400355BR). We thank Zoe Webster and Jane Sealby (Embryonic Stem Cell Facility,
628 MRC Clinical Sciences Centre, Imperial College London) and Paul Sharpe (King's College
629 London) for generation of K14-*Shh* embryos through microinjection. We also thank William
630 Barrell for expertise with schematic diagrams. SO and AB are co-first authors; MTC and SI
631 are co-corresponding authors.

632

References

ADEL AL-LAMI, H., BARRELL, W. B. & LIU, K. J. 2016. Micrognathia in mouse models of ciliopathies. *Biochem Soc Trans,* 44, 1753-1759.

AMANO, T., SAGAI, T., TANABE, H., MIZUSHINA, Y., NAKAZAWA, H. & SHIROISHI, T. 2009. Chromosomal dynamics at the Shh locus: limb bud-specific differential regulation of competence and active transcription. *Dev Cell,* 16, 47-57.

ANDERSON, E., & Hill, R.E. 2014. Long range regulation of the sonic hedgehog gene. *Curr Opin Genet Dev*. 27, 54-9.

BANGS, F. K., SCHRODE, N., HADJANTONAKIS, A. K. & ANDERSON, K. V. 2015. Lineage specificity of primary cilia in the mouse embryo. *Nat Cell Biol,* 17, 113-22.

BILLMYRE, K. K. & KLINGENSMITH, J. 2015. Sonic hedgehog from pharyngeal arch 1 epithelium is necessary for early mandibular arch cell survival and later cartilage condensation differentiation. *Dev Dyn,* 244, 564-76.

BRENT, A. E., SCHWEITZER, R. & TABIN, C. J. 2003. A somitic compartment of tendon progenitors. *Cell,* 113, 235-48.

BRENT, A. E., BRAUN, T. & TABIN, C. J. 2005. Genetic analysis of interactions between the somitic muscle, cartilage and tendon cell lineages during mouse development. *Development,* 132, 515-28.

BRISCOE, J. & THEROND, P. P. 2013. The mechanisms of Hedgehog signalling and its roles in development and disease. *Nat Rev Mol Cell Biol,* 14, 418-31.

CASTILLO, D., SEIDEL, K., SALCEDO, E., AHN, C., DE SAUVAGE, F. J., KLEIN, O. D., & BARLOW, L. A. 2013. Induction of ectopic taste buds by SHH reveals the competency and plasticity of adult lingual epithelium. *Development,* 141, 2993-3002.

CASTILLO-AZOFEIFA, D., SEIDEL, K., GROSS, L., GOLDEN, E. J., JACQUEZ, B., KLEIN, O. D., & BARLOW, L. A. 2018. SOX2 regulation by hedgehog signaling controls adult lingual epithelium homeostasis. *Development,* 145, pii: dev164889.

CHAI, Y., JIANG, X., ITO, Y., BRINGAS, P., JR., HAN, J., ROWITCH, D. H., SORIANO, P., MCMAHON, A. P. & SUCOV, H. M. 2000. Fate of the mammalian cranial neural crest during tooth and mandibular morphogenesis. *Development,* 127, 1671-79.

COBOURNE, M. T., MILETICH, I. & SHARPE, P. T. 2004. Restriction of sonic hedgehog signalling during early tooth development. *Development,* 131, 2875-85.

COBOURNE, M. T., XAVIER, G. M., DEPEW, M., HAGAN, L., SEALBY, J., WEBSTER, Z. & SHARPE, P. T. 2009 Sonic hedgehog signalling inhibits palatogenesis and arrests tooth development in a mouse model of the nevoid basal cell carcinoma syndrome. *Dev Biol*, 331: 38-49.

COBOURNE, M. T., ISEKI, S., BIRJANDI, A. A., ADEL AL-LAMI, H., THAUVIN-ROBINET, C., XAVIER, G. M., & LIU, K. J. 2018. How to make a tongue: Cellular and molecular regulation of muscle and connective tissue formation during mammalian tongue development. *Semin Cell Dev Biol*, 17: 30147-7.

CZAJKOWSKI, M.T., RASSEK, C., LENHARD, D.C., BROHL, D. & BIRCHMEIER, C. 2014. Divergent and conserved roles of Dll1 signalling in development of craniofacial and trunk muscle. *Dev Biol,* 395, 307-16.

DANIELIAN, P. S., ECHELARD, Y., VASSILEVA, G. & MCMAHON, A. P. 1997. A 5.5-kb enhancer is both necessary and sufficient for regulation of Wnt-1 transcription in vivo. *Dev Biol,* 192, 300-9.

DASSULE, H. R., LEWIS, P., BEI, M., MAAS, R. & MCMAHON, A. P. 2000. Sonic hedgehog regulates growth and morphogenesis of the tooth. *Development,* 127, 4775-85.

DU, W., PROCHAZKA, J., PROCHAZKOVA, M. & KLEIN, O. D. 2016. Expression of FGFs during early mouse tongue development. *Gene Expr Patterns,* 20, 81-7.

EVERSON, J. L., FINK, D. M., WON YOON, J., LESLIE, E. J., KIETZMAN, H. W., ANSEN-WILSON, L. J., CHUNG, H. M., WALTERHOUSE, D. O., MARAZITA, M. L. & LIPINSKI, R. J. 2017. Sonic hedgehog regulation of Foxf2 promotes cranial neural crest proliferation and is disrupted in cleft palate morphogenesis. *Development*, 144, 2082-2091.

FENTON, O. M. & Watt-Smith, S. R. 1985. The spectrum of the oro-facial digital syndrome. *Br J Plast Surg*, 38, 532-39.

FERRANTE, M. I., ZULLO, A., BARRA, A., BIMONTE, S., MESSADDEQ, N., STUDER, M., DOLLE, P. & FRANCO, B. 2006. Oral-facial-digital type I protein is required for primary cilia formation and left-right axis specification. *Nat Genet,* 38, 112-17.

FRANCO, B. & THAUVIN-ROBINET, C. 2016. Update on oral-facial-digital syndromes (OFDS). *Cilia,* 5, 12.

FIRULLI, A. B., FUCHS, K. R., VINCENTZ, W. J., CLOUTHIER, E. D., & FIRULLI, B. A. 2014. Hand1 phosphoregulation within the distal arch neural crest is essential for craniofacial morphogenesis. *Development*, 141, 3050-61.

HAN, A., ZHAO, H., LI, J., PELIKAN, R. & CHAI, Y. 2014. ALK5-mediated transforming growth factor beta signalling in neural crest cells controls craniofacial muscle development via tissue-tissue interactions. *Mol Cell Biol,* 34, 3120-31.

HAN, D., ZHAO, H., PARADA, C., HACIA, J. G., BRINGAS, P., JR. & CHAI, Y. 2012. A TGFbeta-Smad4-Fgf6 signalling cascade controls myogenic differentiation and myoblast fusion during tongue development. *Development,* 139, 1640-50.

HAYASHI, S. & MCMAHON, A. P. 2002. Efficient recombination in diverse tissues by a tamoxifen-inducible form of Cre: a tool for temporally regulated gene activation/inactivation in the mouse. *Dev Biol,* 244, 305-18.

HELMS, J. A., BRUGMANN, S. & CORDERO, D. R. 2008. SHH and other genes in the Holoprosencephaly Malformation Sequence. *In: Inborn Errors of Development. The molecular basis of clinical disorders of morphogenesis, Second Edition, Oxford University Press. ISBN-13: 978-019-530691-0,* Edited by Charles J. Epstein, Robert P. Erickson, Anthony Wynshaw-Boris, 291-300

HOSOKAWA, R., OKA, K., YAMAZA, T., IWATA, J., URATA, M., XU, X., BRINGAS, P., JR., NONAKA, K. & CHAI, Y. 2010. TGF-beta mediated FGF10 signalling in cranial neural crest cells controls development of myogenic progenitor cells through tissue-tissue interactions during tongue morphogenesis. *Dev Biol,* 341, 186-95.

HUANGFU, D. & ANDERSON, K. V. 2005. Cilia and Hedgehog responsiveness in the mouse. *Proc Natl Acad Sci U S A,* 102, 11325-330.

INGHAM, P. W. & MCMAHON, A. P. 2001. Hedgehog signalling in animal development: paradigms and principles. *Genes Dev,* 15, 3059-87.

INGHAM, P. W., NAKANO, Y. & SEGER, C. 2011. Mechanisms and functions of Hedgehog signalling across the metazoa. *Nat Rev Genet*, 12, 393-406.

IRIMIA, M., ROYO, J.L., BURGUERA, D., MAESO, I., GÓMEZ-SKARMETA, J.L. & GARCIA-FERNANDEZ, J. 2012. Comparative genomics of the Hedgehog loci in chordates and the origins of Shh regulatory novelties. *Sci Rep.* 2, 433.

IWASAKI, S. 2002. Evolution of the structure and function of the vertebrate tongue. *J Anat,* 201, 1-13.

IWATA, J., SUZUKI, A., PELIKAN, R. C., HO, T. V. & CHAI, Y. 2013. Noncanonical transforming growth factor beta (TGFbeta) signalling in cranial neural crest cells causes tongue muscle developmental defects. *J Biol Chem,* 288, 29760-70.

JEONG, J., MAO, J., TENZEN, T., KOTTMANN, A. H. & MCMAHON, A. P. 2004. Hedgehog signalling in the neural crest cells regulates the patterning and growth of facial primordia. *Genes Dev,* 18, 937-51.

JUNG, H. S., OROPEZA, V. & THESLEFF, I. 1999. Shh, Bmp-2, Bmp-4 and Fgf-8 are associated with initiation and patterning of mouse tongue papillae. *Mech Dev,* 81, 179-82.

LE GUEN, L., NOTARNICOLA, C. & DE SANTA BARBARA, P. 2009. Intermuscular tendons are essential for the development of vertebrate stomach. *Development,* 136, 791-801.

LIU, H. X., MACCALLUM, D. K., EDWARDS, C., GAFFIELD, W. & MISTRETTA, C. M. 2004. Sonic hedgehog exerts distinct, stage-specific effects on tongue and taste papilla development. *Dev Biol,* 276, 280-300.

MARCUCIO, R. S., YOUNG, N. M., HU, D. & HALLGRIMSSON, B. 2011. Mechanisms that underlie co-variation of the brain and face. *Genesis,* 49, 177-89.

MARTINELLI, D. C. &, FAN, C. M. 2007. Gas1 extends the range of Hedgehog action by facilitating its signalling. *Genes Dev*, 21, 1231-1243.

MCMAHON, A. P., INGHAM, P. W. & TABIN, C. J. 2003. Developmental roles and clinical significance of hedgehog signalling. *Curr Top Dev Biol,* 53, 1-114.

MILLINGTON, G., ELLIOT, K. H., CHANG, Y. T., CHANG, C. F., DLUGOSZ, A. & BRUGMANN, S. A. 2017. Cilia-dependent GLI processing in neural crest cells is required for tongue development. *Dev Biol* 424, 124-37.

MIURA, H., SCOTT, J. K., HARADA, S., & BARLOW, L. A. 2014. Sonic hedgehog-expressing basal cells are general post-mitotic precursors of functional taste receptor cells. *Dev Dyn* 243, 1286-97.

MORI-AKIYAMA, Y., AKIYAMA, H., ROWITCH, D. H. & DE CROMBRUGGHE, B. 2003. Sox9 is required for determination of the chondrogenic cell lineage in the cranial neural crest. *Proc Natl Acad Sci U S A,* 100, 9360-5.

MOSES, K. A., DEMAYO, F., BRAUN, R. M., REECY, J. L., & SCHWARTZ, R. J. 2001. Embryonic expression of an Nkx2-5/Cre gene using ROSA26 reporter mice. Genesis, 31, 176-80.

NODEN, D. M. The embryonic origins of avian cephalic and cervical muscles and associated connective tissues. *Am J Anat*, 168, 257-76.

PARADA, C., HAN, D. & CHAI, Y. 2012. Molecular and cellular regulatory mechanisms of tongue myogenesis. *J Dent Res,* 91, 528-35.

PETRYK, A., GRAF, D. & MARCUCIO, R. 2015. Holoprosencephaly: signalling interactions

between the brain and the face, the environment and the genes, and the phenotypic variability in animal models and humans. *Wiley Interdiscip Rev Dev Biol,* 4, 17-32.

RELAIX, F., ROCANCOURT, D., MANSOURI, A. & BUCKINGHAM, M. 2004. Divergent functions of murine Pax3 and Pax7 in limb muscle development. *Genes Dev,* 18, 1088-105.

SAGA, Y., MIYAGAWA-TOMITA, S., TAKAGI, A., KITAJIMA, S., MIYAZAKI, J. & INOUE, T. 1999. MesP1 is expressed in the heart precursor cells and required for the formation of a single heart tube. *Development,* 126, 3437-47.

SAGAI, T., AMANO, T., TAMURA, M., MIZUSHINA, Y., SUMIYAMA, K. & SHIROISHI, T. 2009. A cluster of three long-range enhancers directs regional Shh expression in the epithelial linings. *Development,* 136, 1665-74.

SATIR, P., PEDERSEN, L. B. & CHRISTENSEN, S. T. 2010. The primary cilium at a glance. *J Cell Sci,* 123, 499-503.

SCHWEITZER, R., CHYUNG, J. H., MURTAUGH, L. C., BRENT, A. E., ROSEN, V., OLSON, E. N., LASSAR, A. & TABIN, C. J. 2001. Analysis of the tendon cell fate using Scleraxis, a specific marker for tendons and ligaments. *Development,* 128, 3855-66.

SEPPALA, M., XAVIER, G. M., FAN, C. M. & COBOURNE, M. T. 2014. Boc modifies the spectrum of holoprosencephaly in the absence of Gas1 function. *Biol Open* 8: 728-40.

SONG, Z., LIU, C., IWATA, J., GU, S., SUZUKI, A., SUN, C., HE, W., SHU, R., LI, L., CHAI, Y. & CHEN, Y. 2013. Mice with Tak1 deficiency in neural crest lineage exhibit cleft palate associated with abnormal tongue development. *J Biol Chem,* 288, 10440-50.

SORIANO, P. 1999. Generalized lacZ expression with the ROSA 26 Cre reporter strain. *Nat Genet*, 21, 70-71.

SPOKONY, R. F., AOKI, Y., SAINT-GERMAIN, N., MAGNER-FINK, E. & SAINT-JEANNET, J. P. 2002. The transcription factor Sox9 is required for cranial neural crest development in Xenopus. *Development,* 129, 421-32.

SUBRAMANIAN, A. & SCHILLING, T. F. 2015. Tendon development and musculoskeletal assembly: emerging roles for the extracellular matrix. *Development,* 142, 4191-204.

SUKEGAWA, A., NARITA, T., KAMEDA, T., SAITOH, K., NOHNO, T., IBA, H., YASUGI, S. & FUKUDA, K. 2000. The concentric structure of the developing gut is regulated by Sonic hedgehog derived from endodermal epithelium. *Development,* 127, 1971-80.

TAPADIA, M. D., CORDERO, D. R. & HELMS, J. A. 2005. It's all in your head: new insights into craniofacial development and deformation. *J Anat,* 207, 461-77.

792 ULLOA, F. & BRISCOE, J. 2007. Morphogens and the control of cell proliferation and
793 patterning in the spinal cord. *Cell Cycle,* 6, 2640-49.
794 XAVIER, G. M., SEPPALA, M., BARRELL, W., BIRJANDI, A. A., GEOGHEGAN, F. & COBOURNE,
795 M.T. 2016. Hedgehog receptor function during craniofacial development. *Dev Biol* 415:
796 198-215.
797 XU, J., LIU, H., LAN, Y., ADAM, M., CLOUTHIER, D. E. , POTTER, S., & JIANG, R. 2019.
798 Hedgehog signalling patterns the oral-aboral axis of the mandibular arch. *eLife*, pii:
799 e40315.
800 ZHU, X. J., YUAN, X., WANG, M., FANG, Y., LIU, Y., ZHANG, X., YANG, X., LI, Y., LI, J., LI, F., DAI, Z.
801 M., QIU, M., ZHANG, Z. & ZHANG, Z. 2017. A Wnt/Notch/Pax7 signalling network
802 supports tissue integrity in tongue development. *J Biol Chem*, 292, 9409-19.
803

Figure legends

Figure 1 Reduced SHH signalling in lingual epithelium results in impaired myotubule arrangement

(A-F) mRNA ISH of *Shh* (A, B), *Ptch1* (C, D), *Gli1* (E, F), *Myf5* (G, H) on sagittal sections of the developing tongue in WT (A, C, E) and $Shh^{MFCS4/-}$ (B, D, F) heads at E11.5 (anterior is to the left for A-H). (Ia-Lp) mRNA ISH of *Myod1* (Ia-Jp) and IHC for desmin (Ka-Lp) on coronal sections of the developing tongue in WT (Ia, Ja; Ka, La) and $Shh^{MFCS4/-}$ (Ip, Jp; Kp, Lp) heads at E11.5. Coronal plane of section indicated in G, H is (a) anterior and (p) posterior for Ia-Lp. Scale bar for A-L is in H. (M) Semi-quantitative RT-PCR analysis of *Shh*, *Ptch1*, *Gli1*, and *Myf5* transcription in WT and $Shh^{MFCS4/-}$ tongue at E11.5. (N-Q) Expression of *Myod1* and IHC for desmin on coronal sections of E13.5 WT (N, P) and $Shh^{MFCS4/-}$ (O, Q). Scale bar for N-Q is in Q. (R-U) IHC for SMA on coronal sections of P0 WT (R, T) and $Shh^{MFCS4/-}$ (S, U) tongues. Area of the lingual septum (white boxes) is highlighted in T, U. Scale bar for R, S is in S and T, U is in U. A-J and N, O are all digoxigenin-labelled ISH. gg, genioglossus; il/v/tv, inferior longitudinal, vertical and transverse muscle; m, mandible; sg, styloglossus muscle; sl, superior longitudinal muscle; t, tongue.

Figure 2 SHH signalling is required for differentiation of lingual CNCC to tenocytes

(A-H) mRNA ISH of *Scx* on coronal sections of the developing tongue (A-D, G, H) and in whole mount (E, F) at E11.5 (A, B), E12.5 (C-F) and E13.5 (G, H) in WT (A, C, E, G) and $Shh^{MFCS4/-}$ (B, D, F, H) embryos. *Scx* expression in the future aponeurosis and lingual septum indicated by arrows and the dotted line in A, C, E, and G, which is not consecutive in $Shh^{MFCS4/-}$ (arrows in D, F, H). Arrowheads in (G, H) indicate the short genioglossus (g) tendon origins at the paired superior mental spines. Scale bar for A-D, G, and H in H; for E, F

in F. (I, J) mRNA ISH of *Sox9* at E12.5 on coronal sections of the developing tongue in WT (I) and $Shh^{MFCS4/-}$ (J) embryos (arrow in I indicates expression in the future lingual septum). (K-N) mRNA ISH of *Col1a1* (K, L) and *Fn1* (M, N) at E13.5 on coronal sections of the developing tongue in WT (K, M) and $Shh^{MFCS4/-}$ (L, N) embryos. Scale bar for I, J in J and for K-N in N. (O) Lingual CNCC-derived and mesoderm-derived mesenchymal cell proliferation index at E11.5 and E12.5 in WT and $Shh^{MFCS4/-}$ embryos. *P*-values for each pair were 0.14, 0.051, 0.26, and 0.25, respectively.

Figure 3 Temporal loss of *Shh* produces a graded effect on tongue development

(A-D) H+E stained coronal histological analysis of the developing tongue in (A) E14.5 WT and (B-D) $pCag\text{-}CreER^{TM}; Shh^{flox/flox}$ embryos injected with tamoxifen at E10.5, E11.5, E12.5 and harvested at E14.5, respectively. (E-H) Intrinsic muscle organization in the tongue dorsum identified within the black rectangles in A-D. (I-P) mRNA ISH of *Myod1* (I-L) and *Scx* (M-P) on WT (I, M) and $pCag\text{-}CreER^{TM}; Shh^{flox/flox}$ embryos that received tamoxifen at E10.5, E11.5, E12.5 and harvested at E14.5 (J, N; K, O; L, P; respectively). *Scx* expression in WT embryos at E14.5 is highlighting the lingual septum (M, arrow); genioglossus (small arrowhead) and geniohyoid muscles (large arrowhead). Scale bar in P for A-D and I-P; in H for E-H.

Figure 4 SHH signalling is received by CNCC for tendon formation and myotube arrangement

(A-E) CNCC-derived mesenchyme visualized in the developing tongue by X-gal staining for beta-galactosidase activity on coronal (A) and sagittal (B, C) sections of E12.5 *Wnt1-Cre; R26R* embryos (C is a magnified view of the boxed area in B). (D, E) SHH responsive cells and mesodermal cells were determined by ISH expression analysis on sections adjacent to B

(and corresponding to region C) for *Ptch1* (D) and *Myf5* (E), respectively (arrows in D, E indicate superior longitudinal muscles in C, D, E). Scale bar in B for A, B; and in E for C-E. (F-K) SHH signal activity was studied by mRNA ISH for *Ptch1* expression on sagittal sections of E11.5 (F-H) and E12.5 (I-K) WT (F, I), *Wnt1-Cre; Ofd*$^{fl/Y}$ (G, J) and *Mesp1-Cre; Ofd*$^{fl/Y}$ (H, K) embryos. (L-N) Lingual myotube arrangement was examined by mRNA ISH for *Myod1* on coronal sections of E13.5 WT (L), *Wnt1-Cre; Ofd*$^{fl/Y}$ (M), and *Mesp1-Cre; Ofd*$^{fl/Y}$ (N). Scale bar in H for F-H, in K for I-N. m, mandibular process; t, tongue; ht, heart; ps, palatal shelf.

Figure 5 TGFβ signalling is downstream of SHH in the developing tongue

(A-F) *Tgfb1, -2,* and *-3* , and *Fgfr1* expression on coronal sections of E13.5 WT (A, C, E, I) and *Shh*$^{MFCS4/-}$ (B, D, F, J) oral region. *Tgfb3* and *Fgfr1* transcription in the lingual septum was indicated by arrow. Scale bar in F for A-F, I, and J. (G) pSMAD2/3 was studied in the tongue of WT and *pCag-CreER*^{TM}*; Shh*$^{flox/flox}$ embryos (mutant) injected with tamoxifen at E10.5 and harvested 3 days later. WB detection for pSMAD2/3 is in G. The band intensity was analysed statistically. *** for $p<0.01$ significance. (H) *Fgfr1* transcription in the tongue was evaluated in the WT and *Shh*$^{MFCS4/-}$ by semi-quantitative PCR.

Figure 6 Schematic representation of SHH function during murine tongue development

(A-E) SHH signalling during normal and abnormal tongue development. The upper panels represent SHH signal transduction in the early tongue at E11.5 in WT and mutant mice analysed in this investigation, with the lower panels representing subsequent tongue development at E14.5. (A) In WT mice, SHH signals from the early tongue, pharyngeal and laryngeal epithelium to underlying CNCC and is required for normal formation of the lingual

879 tendon and intrinsic muscle patterning; (B) *MFCS4*$^{-/-}$ mice have downregulated SHH in the
880 pharyngeal and laryngeal regions with soft palate truncation, deformation of the posterior
881 tongue and loss of the epiglottis; (C) *Shh*$^{MFCS4/-}$ mice have an almost complete loss of SHH in
882 the developing tongue and pharyngeal region with lack of lingual septum tendon,
883 disorganized intrinsic muscles, hypoglossia and cleft palate; (D) *pCag-Cre; Shh*$^{fl/fl}$ have loss
884 of SHH throughout the craniofacial region from E10.5, including the tongue, and have
885 absence of the lingual tendon, disorganized intrinsic muscles, hypoglossia, micrognathia and
886 cleft palate; (E) *Wnt1-Cre; Ofd*$^{fl/Y}$ mice have a reduced SHH signal response in CNCC with
887 hypoglossia, clefting of the tongue with poorly organized clumps of intrinsic muscles, cleft
888 palate and micrognathia. (For A-E, *Shh* expression in red, *Ptch1* CNCC expression in purple,
889 lingual tendon in green, extrinsic tongue muscles are curved grey lines, normal intrinsic
890 muscles are vertical grey lines with pink background, disrupted intrinsic muscles are grey
891 crosses with pink background. CP, cleft palate; e, epiglottis; h, hyoid bone; m, mandibular
892 process; ms, mandibular symphysis; sp, soft palate; t, tongue). (F) Temporal requirements for
893 SHH function in tongue development. Key stages of early tongue development in the
894 developing embryo at E9.5, E11.5 and E13.5 (SHH in red, CNCC in blue, myogenic
895 progenitors and intrinsic/extrinsic tongue musculature in pink and lingual tendon in green).
896 SHH from the tongue epithelium is required for the specification and differentiation of
897 tenocytes from CNCC. Formation of the lingual tendon (green) provides a scaffold for
898 myoblast cell populations, which facilitates normal patterning of the intrinsic musculature.
899
900
901

902 Supplementary files

903 **Supplemental figure 1 mRNA ISH of *Shh* and *Ptch1* in the developing mandibular**

arch and tongue

(A-D) Sagittal sections through the approximate midline of the first mandibular arch in (A, B) E10.5 and (C, D) E11.5 mouse embryos. *Shh* is expressed in the oropharyngeal and pharyngeal endoderm at E10.5, extending into the pharyngeal epithelium of the early tongue by E11.5. *Ptch1* expression extends into the mandibular arch and entirety of the early tongue mesenchyme at these corresponding time-points. (E-J) Coronal sections through the developing tongue at (E, F) E11.5, (G, H) E12.5, and (I, J) E13.5. *Shh* expression becomes progressively restricted from throughout the epithelium to the fungiform papilla during tongue development; however, whilst also becoming restricted *Ptch1* expression is still present throughout the underlying mesenchyme, albeit in a reduced gradient of activity, despite restriction of *Shh* to the fungiform papillae. Black arrows indicate oropharyngeal endoderm, paired black arrowheads indicate pharyngeal endoderm, blue arrowhead indicates the border between the developing tongue and mandible, * indicates fungiform papillae (m, mandible; md, mandibular arch; t, tongue).

Supplemental figure 2 Disorganization of tongue muscle arrangement was rarely observed in *Shh*$^{MFCS4/MFCS4}$ embryos

(A-D) H+E staining (A, B) and IHC for desmin (C, D) on frontal sections of WT (A, C) and *Shh*$^{MFCS4/MFCS4}$ embryos (B, D) at E15.5. Arrow points the lingual septum, Scale bar in D for A-D.

Supplemental figure 3 Abnormal tongue formation induces cleft palate

(A-F) H+E staining on frontal sections of WT (A, C, E) and *Shh*$^{MFCS4/-}$ (B, D, F) embryos at E13.0 (A, B), E14.0 (C, D) and E14.5 (E, F). ps: palatal shelf, t; tongue. Scale bar is in F. (G, H) Aboral view of the secondary palate after organ culture of E13.5 for 24 hours maxilla of

929 WT (G) and *Shh*$^{MFCS4/-}$ (H). Scale bar is in H.

930

931 **Supplemental figure 4 Vascularization or innervation is not affected in *Shh*$^{MFCS4/-}$**
932 **mice**

933 (A, B) Immunofluorescent detection of an endothelial marker CD31 (green) on E13.5 coronal
934 sections of WT (A) and the *Shh*$^{MFCS4/-}$ (B). (C, D) Immunofluorescent detection of the neuron
935 marker synaptophysin (green) on E13.5 coronal sections of WT (C) and the *Shh*$^{MFCS4/-}$ (D).
936 Nuclei were stained blue by Hoechst. Scale bar in D for A-D.

937

938 **Supplemental figure 5 Intrinsic muscle organization in the tongue is dependent**
939 **upon timing of SHH signal loss**

940 (A-D) Frontal analysis of the developing tongue in (A) E14.5 WT and (B-D) *pCag-CreER*^{TM}*;*
941 *Shh*$^{flox/flox}$ embryos injected with tamoxifen at (B) E10.5, (C) E11.5, (D) E12.5 and harvested
942 at 4, 3, 2 days later, respectively. Dewaxed frontal sections of the tongue dorsum imaged
943 under fluorescence to highlight intrinsic muscle fibres (white arrowheads).

944

945 **Supplemental figure 6 SHH co-receptor expression in *Shh*$^{MFCS4/-}$ embryonic tongue**

946 (A-D, F-I) mRNA ISH for *Gli1* (A), *Ptch1* (B), *Ptch2* (C), *Myf5* (D), *Hhip* (F), *Gas1* (G),
947 *Cdon* (H), and *Boc* (I) with X-gal staining (E) on the sagittal section of the equivalent
948 position at E11.5. m; mandible; mc, mesenchymal core; t, tongue. Scale bar in I for A-I.

949

950 **Supplemental figure 7 TGFβ signalling is influenced by SHH in the developing**
951 **tongue but WNT signalling is not**

952 (A, B) Semi-quantitative RT-PCR analysis of *Tgfb1*, *-2*, *-3*, and *Axin2* transcription in the
953 tongue of the WT and the *Shh*$^{MFCS4/-}$ at E12.5. (C, D) mRNA ISH of *Axin2* on sagittal section

954 of WT (C) and *pCag-CreER*^{TM}*; Shh*$^{flox/flox}$ embryos injected with tamoxifen at E10.5 and were

955 harvested 4 days later (D).

956

957

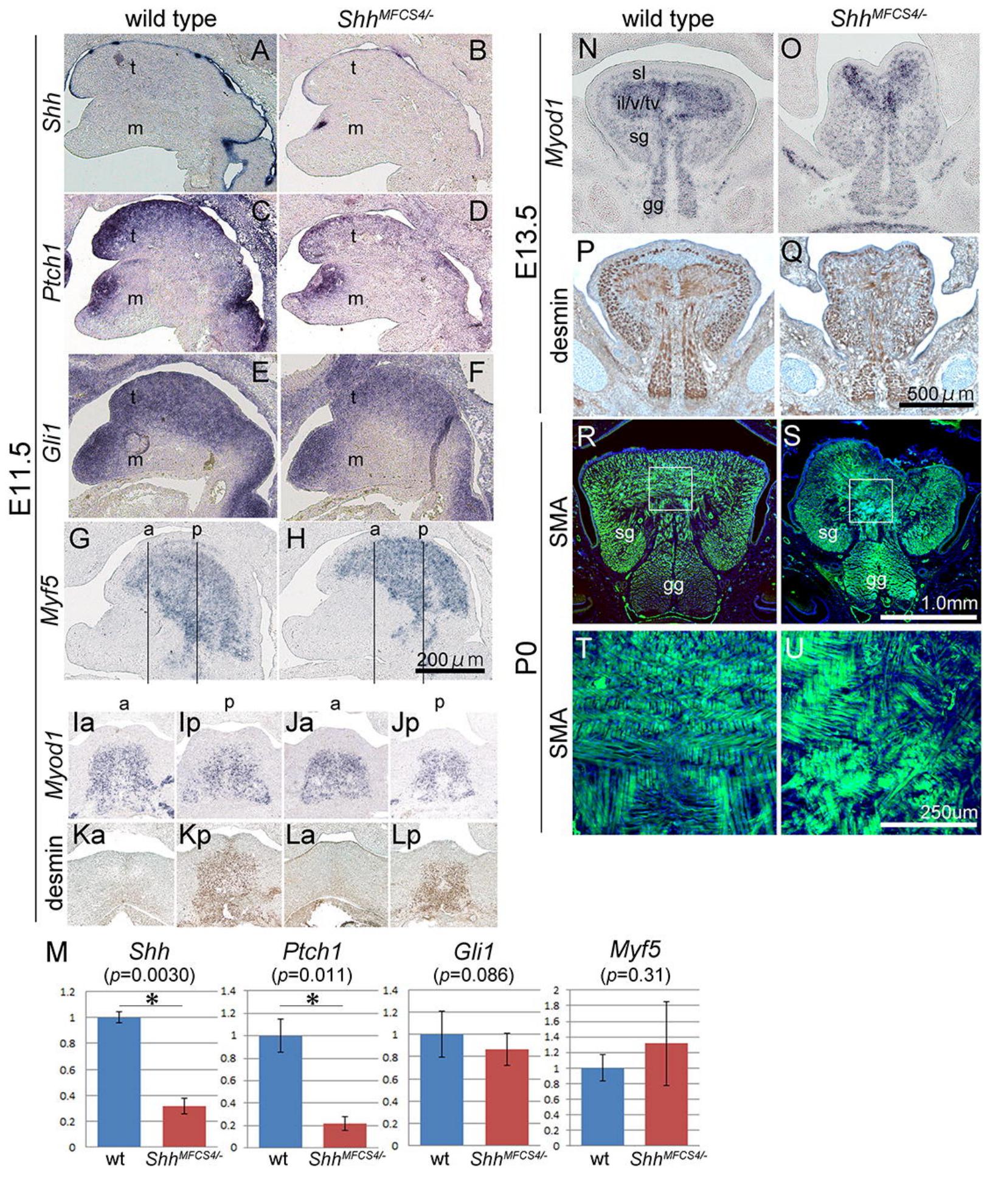
wild type
Shh^MFCS4/-
wild type
Shh^MFCS4/-
E11.5
E13.5
P0
Shh
Ptch1
Gli1
Myf5
Myod1
desmin
SMA
SMA
A
B
C
D
E
F
G
H
N
O
P
Q
R
S
T
U
Ia
Ip
Ja
Jp
Ka
Kp
La
Lp
t
m
a
p
sl
il/v/tv
sg
gg
200 μm
500 μm
1.0mm
250um
M
Shh
(p=0.0030)
Ptch1
(p=0.011)
Gli1
(p=0.086)
Myf5
(p=0.31)
*
*
wt
Shh^MFCS4/-

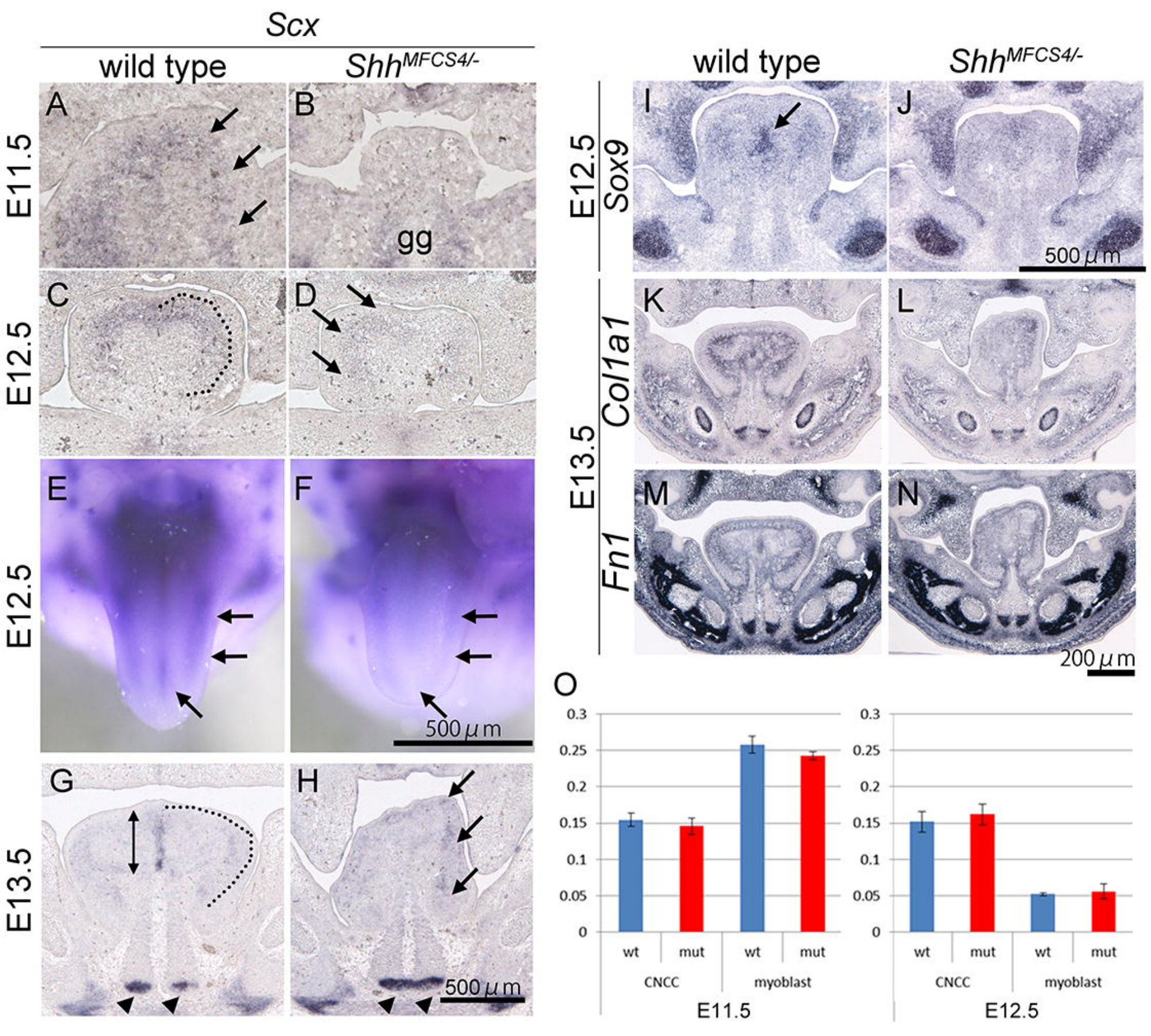
Scx
wild type
Shh^MFCS4/-
A
B
gg
E11.5
C
D
E12.5
E
F
500 μm
E12.5
G
H
500 μm
E13.5
wild type
Shh^MFCS4/-
I
J
500 μm
E12.5
Sox9
K
L
Col1a1
M
N
200 μm
E13.5
Fn1
O
0.3
0.25
0.2
0.15
0.1
0.05
0
wt
mut
wt
mut
CNCC
myoblast
E11.5
E12.5

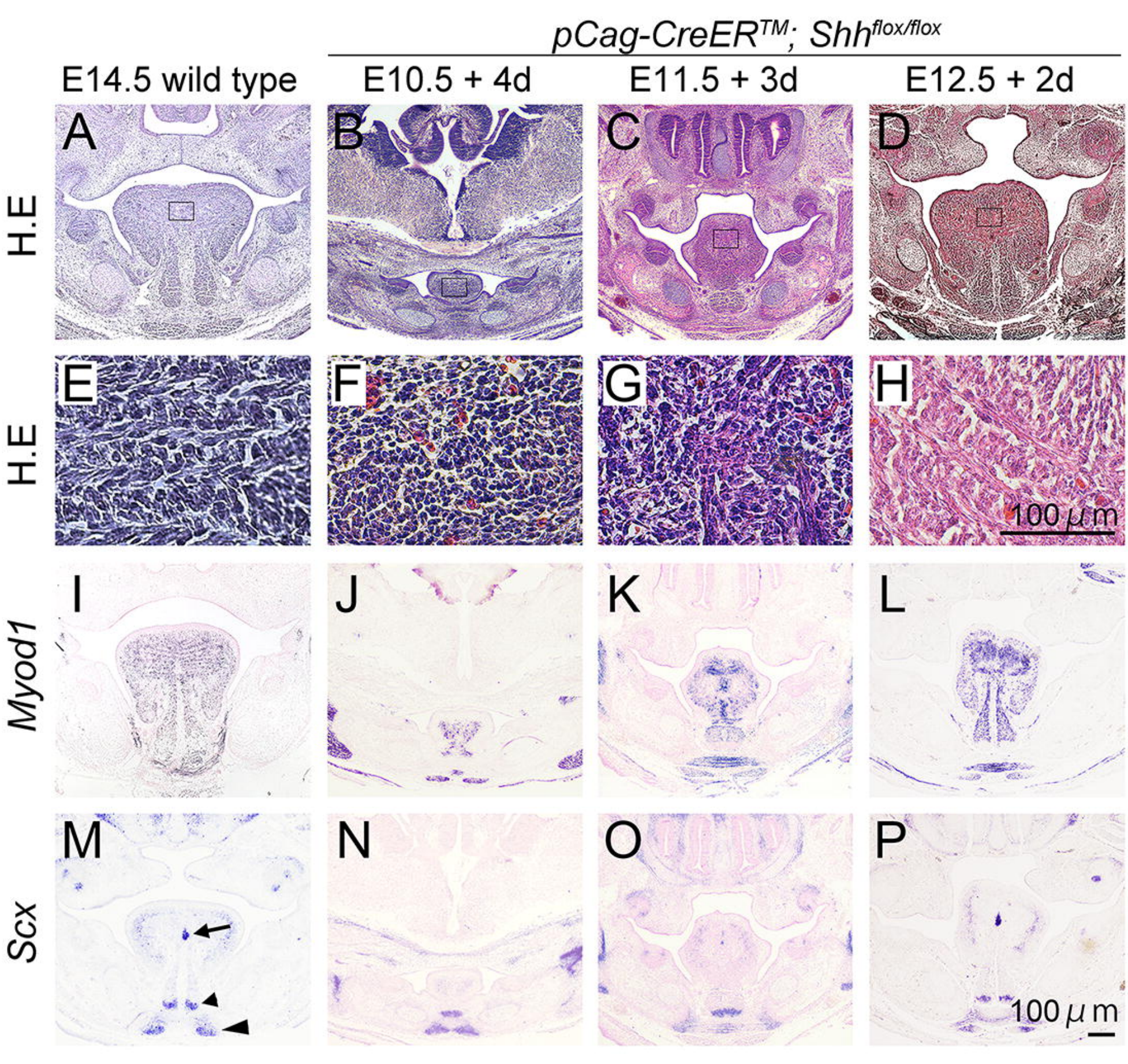
pCag-CreER™; Shh flox/flox
E14.5 wild type
E10.5 + 4d
E11.5 + 3d
E12.5 + 2d
H.E
H.E
Myod1
Scx
A
B
C
D
E
F
G
H
I
J
K
L
M
N
O
P
100 μm
100 μm

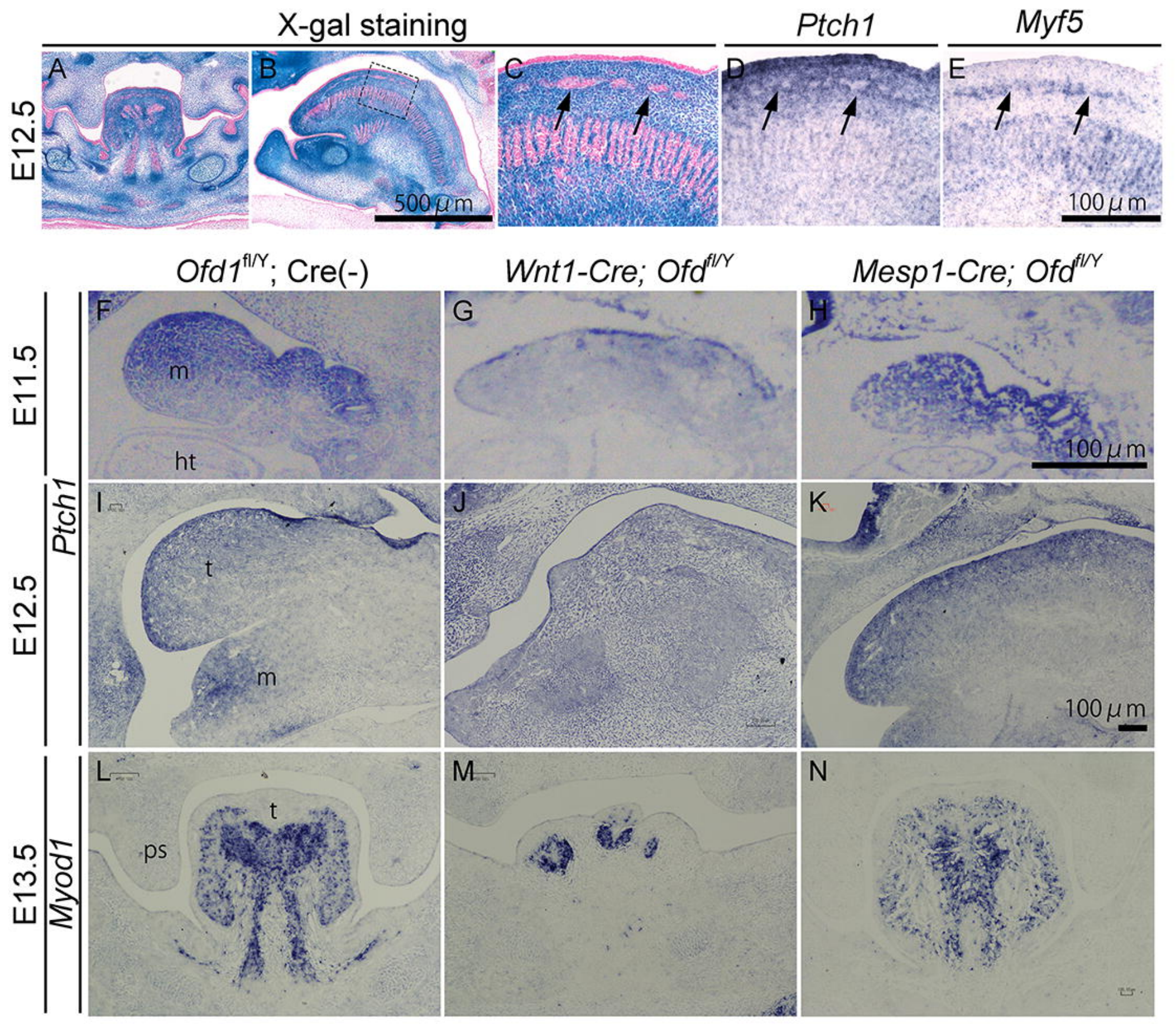
X-gal staining
Ptch1
Myf5
E12.5
A
B
C
D
E
500 μm
100 μm
Ofd1fl/Y; Cre(-)
Wnt1-Cre; Ofdfl/Y
Mesp1-Cre; Ofdfl/Y
E11.5
Ptch1
E12.5
E13.5
Myod1
F
G
H
I
J
K
L
M
N
m
ht
t
m
t
ps
100 μm

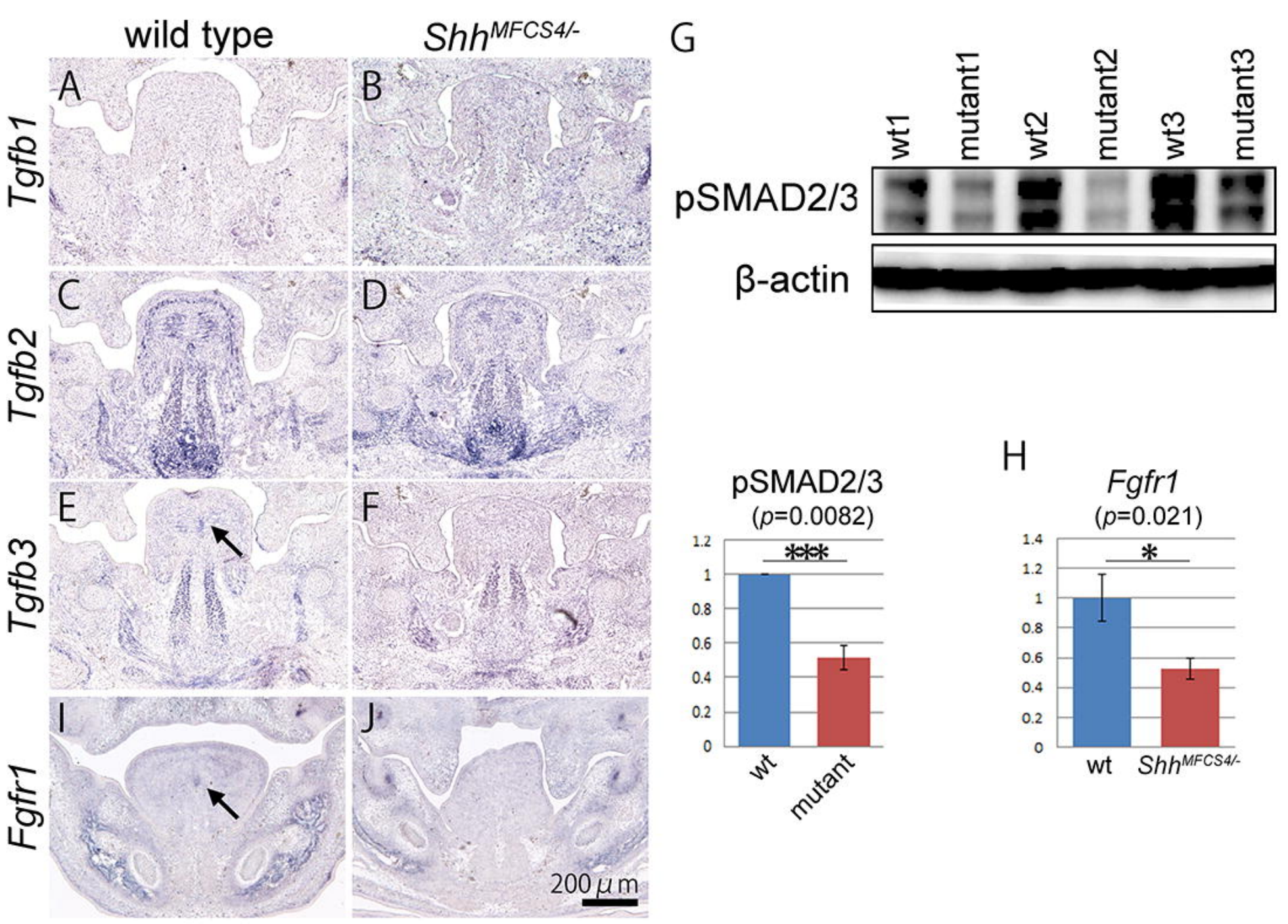
wild type
Shh^MFCS4/-
A
B
C
D
E
F
I
J
Tgfb1
Tgfb2
Tgfb3
Fgfr1
200 μm
G
wt1
mutant1
wt2
mutant2
wt3
mutant3
pSMAD2/3
β-actin
pSMAD2/3
(p=0.0082)
***
wt
mutant
H
Fgfr1
(p=0.021)
*
wt
Shh^MFCS4/-

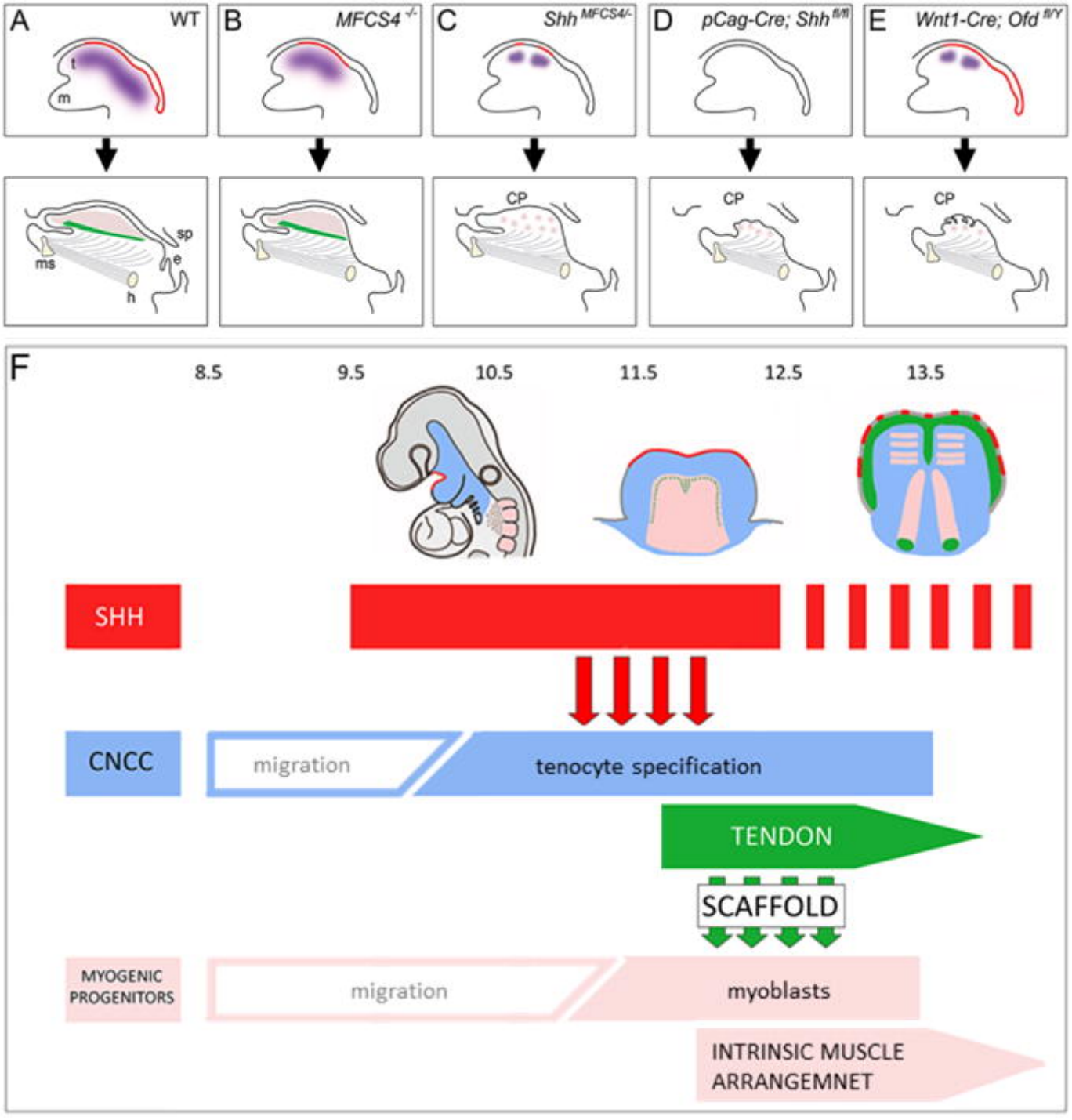
A
WT
t
m
B
MFCS4 -/-
C
Shh MFCS4/-
D
pCag-Cre; Shh fl/fl
E
Wnt1-Cre; Ofd fl/Y
sp
e
ms
h
CP
CP
CP
F
8.5
9.5
10.5
11.5
12.5
13.5
SHH
CNCC
migration
tenocyte specification
TENDON
SCAFFOLD
MYOGENIC PROGENITORS
migration
myoblasts
INTRINSIC MUSCLE ARRANGEMNET